FACULTY OF CHEMISTRY

DEPARTMENT OF PHYSICAL CHEMISTRY AND TECHNOLOGY OF POLYMERS

Functionalized organic coatings as bioelectronic interfaces

Funkcjonalizowane pokrycia organiczne jako interfejsy bioelektroniczne

mgr inż. Małgorzata Bogusz

Supervisor: dr hab. inż. Katarzyna Krukiewicz, prof. PŚ

Gliwice, 2025

Table of contents

Abstract

The advancement of implantable bioelectronic devices holds significant promise for applications in neural engineering, biosensing, and electroceutical therapies. However, the long-term performance and integration of these devices are critically dependent on several characteristics, such as electrochemical properties, biocompatibility, and functional adaptability of the electrode-tissue interface. The aim of this thesis was to develop and investigate advanced surface functionalization strategies to enhance these key characteristics, with a key focus on electrochemical modification methods, incorporating conducting polymers, deposition of metal particles, and electrografting of diazonium salts. These methods were further complemented by secondary surface treatments, including physical approaches such as solvent treatment, and chemical strategies like covalent coupling. All proposed functionalization methods were followed by comprehensive characterization of relevant parameters, such as morphology, electrical and electrochemical performance, biocompatibility, and antibacterial properties.

The research presented in this thesis contributes to the growing library of surface functionalization strategies for bioelectronic devices. By offering tailored solutions to meet diverse functional requirements, these approaches support the development of more efficient and adaptable material interfaces. Given the rapid growth of the bioelectronics market and its increasing demand for high-performance, biocompatible, and multifunctional materials, such advancements are particularly valuable for accelerating innovation in next-generation implantable bioelectronic devices.

Streszczenie

Rozwój wszczepialnych urządzeń bioelektronicznych budzi duże nadzieje w kontekście zastosowań w inżynierii tkanki nerwowej, biosensorach i terapiach elektroceutycznych. Długoterminowa wydajność oraz skuteczna integracja z mikrośrodowiskiem biologicznym są w dużej mierze zależne od takich parametrów jak właściwości elektrochemiczne, biokompatybilność oraz zdolność do funkcjonalnego dostosowania interfejsu elektroda-tkanka. Celem niniejszej pracy było opracowanie i zbadanie zaawansowanych strategii funkcjonalizacji powierzchni, mających na celu poprawę tych kluczowych cech, ze szczególnym uwzględnieniem elektrochemicznych metod modyfikacji, obejmujących zastosowanie polimerów przewodzących, osadzanie cząstek metalu i elektroszczepienie soli diazoniowych. Zastosowane podejścia uzupełniono dodatkowymi metodami obróbki powierzchni: fizycznymi (takimi jak domieszkowanie wtórne za pomocą rozpuszczalników) oraz chemicznymi (m.in. sprzęganie kowalencyjne). Wszystkie zaproponowane techniki funkcjonalizacji zostały poddane kompleksowej charakterystyce, obejmującej analizę morfologii, właściwości elektrycznych i elektrochemicznych, biokompatybilności oraz aktywności przeciwbakteryjnej.

Przedstawione w pracy badania poszerzają zakres dostępnych rozwiązań w obszarze funkcjonalizacji materiałów dla bioelektroniki. Proponując dostosowane rozwiązania ukierunkowane na spełnienie różnorodnych wymagań funkcjonalnych, przyczyniają się one do rozwoju bardziej wydajnych i adaptowalnych materiałów interfejsowych. W obliczu dynamicznego rozwoju rynku bioelektroniki oraz rosnącego zapotrzebowania na zaawansowane, biokompatybilne i wielofunkcyjne materiały, przedstawione rozwiązania mogą odegrać istotną rolę w przyspieszeniu innowacji w obszarze nowej generacji implantowalnych urządzeń bioelektronicznych.

List of publications

The presented doctoral thesis is based on a series of 7 thematically related papers listed below. Their full texts, together with supplementary information, can be found in the **Appendix** section at the end of this dissertation.

[A1] **M. Skorupa**, D. Więcławska, D. Czerwińska-Główka, M. Skonieczna, K. Krukiewicz, Dopant-Dependent Electrical and Biological Functionality of PEDOT in Bioelectronics, Polymers (Basel). 13 (2021) 1948. https://doi.org/10.3390/polym13121948.

MNiSW = 100; IF = 5.0.

[A2] S. Smołka, **M. Skorupa**, K. Fołta, A. Banaś, K. Balcerzak, D. Krok, D.Y. Shyntum, M. Skonieczna, R. Turczyn, K. Krukiewicz, Antibacterial coatings for electroceutical devices based on PEDOT decorated with gold and silver particles, Bioelectrochemistry. 153 (2023) 108484. https://doi.org/10.1016/j.bioelechem.2023.108484.

MNiSW = 100; IF = 4.8.

[A3] **M. Skorupa**, K. Karoń, E. Marchini, S. Caramori, S. Pluczyk-Małek, K. Krukiewicz, S. Carli, PEDOT:Nafion for Highly Efficient Supercapacitors, ACS Appl. Mater. Interfaces. 16 (2024) 23253–23264. https://doi.org/10.1021/acsami.4c01085.

MNiSW = 200; IF = 8.5.

[A4] **M. Skorupa**, E. Cao, A. Barylski, S. Shakibania, S. Pluczyk-Małek, Z. Siwy, K. Krukiewicz, Layer-By-Layer Approach to Improve the Capacitance of Conducting Polymer Films, Adv. Electron. Mater. 2400761 (2025) 1–11. https://doi.org/10.1002/aelm.202400761.

MNiSW = 140; IF = 5.3.

[A5] S. Smołka, **M. Skorupa**, A. Barylski, M. Basiaga, K. Krukiewicz, Improved adhesion and charge transfer between PEDOT:PSS and the surface of a platinum electrode through a diazonium chemistry route, Electrochem. Commun. 153 (2023) 107528. https://doi.org/10.1016/j.elecom.2023.107528.

MNiSW = 100; IF = 4.7.

[A6] **M. Skorupa**, M. Skonieczna, D.Y. Shyntum, Abdullah, R. Turczyn, M. Asplund, K. Krukiewicz, Electrografted mixed organic monolayers as antibacterial coatings for implantable biomedical devices, Electrochim. Acta. 492 (2024) 144354. https://doi.org/10.1016/j.electacta.2024.144354.

MNiSW = 100; IF = 5.5.

[A7] T. Patel, **M. Skorupa**, M. Skonieczna, R. Turczyn, K. Krukiewicz, Surface grafting of poly-L-lysine via diazonium chemistry to enhance cell adhesion to biomedical electrodes, Bioelectrochemistry. 152 (2023) 108465. https://doi.org/10.1016/j.bioelechem.2023.108465.

MNiSW = 100; IF = 4.8.

Nomenclature

ITO	indium tin oxide
AC	alternating current
ACN	acetonitrile
AFM	atomic force microscopy
AG	ageing
B35	rat neuroblastoma cell line
Bu_4NBF_4	tetrabutylammonium tetrafluoroborate
Bu_4NPF_6	tetrabutylammonium hexafluorophosphate
C	capacitance
CP	conducting polymer
CSC	charge storage capacity
CV	cyclic voltammetry
DC	direct current
D-Cl_2	3,5-dichlorophenyldiazonium tetrafluoroborate
DMSO	dimethyl sulfoxide
DNA	deoxyribonucleic acid
D-NH_2	4-aminophenyl
D-NO_2	4-nitrobenzenediazonium tetrafluoroborate
D-OCH_3	4-methoxydiazonium tetrafluoroborate
E. coli	*Escherichia coli*
EDC	1-ethyl-3-(3-dimethylaminopropyl)carbodiimide
EDOP	3,4-ethylenedioxypyrrole
EDOT	3,4-ethylenedioxythiophene
EDS	energy dispersive X-ray spectroscopy
EG	ethylene glycol
EIS	electrochemical impedance spectroscopy
FIB	focused ion beam
FTIR	Fourier transform infrared spectroscopy
GCD	galvanostatic charge–discharge
I_{rel}	relative anodic peak current
Lc	critical load
MTT	3-[4,5-dimethylthiazol-2-yl]-2,5-diphenyltetrazolium bromide
NHDF	normal human dermal fibroblasts
PBS	phosphate-buffered saline
PEDOP	poly(3,4-ethylenedioxypyrrole)

PEDOT	poly(3,4-ethylenedioxythiophene)
PLL	poly-L-lysine
PSS	poly(4-styrene sulfonate)
pTS	p-toluene sulfonate
R_{ct}	charge transfer resistance
S_a	roughness parameter, arithmetic mean height
SEM	scanning electron microscopy
SH-SY5Y	human neuroblastoma cell line
US	ultrasound

1. Introduction

Electroactive interfaces between living cells and electronic systems are fundamental to bioelectronic applications, which depend on efficient communication between living cells and artificial components. This strategy enables controlled, bidirectional information exchange, allowing external electronic devices to directly interact with living matter [8]. It plays a critical role in biomedical applications such as biosensors, tissue engineering, and neuroprosthetics [9], supporting functions like sensing, stimulation, or modulation of cellular activity. A seamless connection between biotic and abiotic systems requires well-designed interfacing platforms. Consequently, interfacial materials should be able to deliver electrical signals to cells, exhibit low impedance, a suitable surface topography, and biocompatibility.

The well-established and widely used materials for the construction of bioelectronic devices are noble metals. Gold is frequently applied in electrochemical biosensors and microelectrode arrays [10]. The application of iridium and iridium oxide lies primarily in high-current stimulation and stimulation electrode arrays, neural recording, and retinal implants [11]. But above all, platinum has historically been the main material of choice in commercial devices for neural stimulation and recording, such as cochlear implants, deep brain stimulation electrodes, or pacemakers [12,13]. These materials exhibit several advantages, such as high conductivity, biocompatibility, chemical stability, and corrosion resistance. However, they come with several limitations that include high impedance in small sized electrodes, limited charge injection capacity, and potential for corrosion and tissue damage at high stimulation levels [13]. Additionally, their mechanical mismatch and lack of integration with soft biological tissue contribute to inflammation, glial scar formation, and as a result – reduced device performance over time [14]. Moreover, the surface biocompatibility of noble metals also applies to prokaryotic organisms, leading to increased risk of implant-associated bacterial infections [15].

Consequently, to improve the performance of metal-based bioelectronic devices and enhance their interaction with biological systems, surface modification techniques are essential. These modifications can be achieved through physical, chemical, or combined approaches. Physical methods, such as laser-based micropatterning, increase surface roughness to promote cell adhesion [16]. In contrast, chemical methods focus on enhancing biological affinity by functionalizing the surface with conductive polymers [17,18], peptides [19,20], or adhesion-promoting molecules [21]. Among the surface functionalization techniques, electrochemical surface modification has emerged as a powerful and versatile approach for the fabrication of bioelectronic platforms, primarily due to their simplicity, cost-effectiveness, high efficiency, and precise controllability over the deposition parameters. A key advantage of these methods is the ability to monitor and regulate the deposition process in real-time through *in situ* electrochemical measurements [22]. In an electrochemical

deposition process, the application of an electric stimulus across an electrolytic solution initiates reduction and/or oxidation reactions at the surface of a working electrode. These redox reactions drive the nucleation and growth of a thin film of the target material, which can be either inorganic (e.g. metals, metal oxides) or organic (e.g. conducting polymers, biomolecules). The resulting deposited layer can significantly modify the surface morphology, chemical composition, electrical conductivity, and biocompatibility of the substrate, therefore enabling its functional integration into bioelectronic devices [23,24].

2. Hypothesis and research objectives

In my research, I hypothesized that surface functionalization of electrodes using conducting polymers, metal particles, and diazonium-based modifications – individually or in combination – can be employed to enhance the electrochemical performance, biocompatibility, and application-specific functionality of implantable bioelectronic interfaces.

Accordingly, I formulated the following research objectives:

1. To develop a series of electroactive surface coatings for implantable bioelectronic devices using conducting polymers, metal particles, and diazonium electrografting.
2. To investigate secondary surface modification techniques, such as solvent treatment, layer-by-layer deposition and chemical coupling, aimed at enhancing selected material properties.
3. To characterize the physicochemical and electrochemical properties of the modified surfaces using microscopy, spectroscopy, and electroanalytical techniques.
4. To evaluate the biocompatibility and antibacterial activity of the functionalized coatings through *in vitro* cell culture and microbial assays.
5. To establish structure–function relationships linking surface functionalization strategies with improved interface performance.
6. To define strategic approaches for surface functionalization, enabling the development of multifunctional and biocompatible coatings that meet the application-specific requirements of implantable bioelectronic devices.

The disclosed research outcomes have been published in peer-reviewed international scientific journals. The doctoral dissertation presents a summary of the most important results, with a particular focus on the parts that I have personally worked on during my PhD.

3. Methodology

3.1. Investigated surfaces

The experiments conducted within this thesis were focused on modifications of platinum surfaces **[A1, A2, A4, A5, A6, A7]**, as well as glass slides covered with indium tin oxide (ITO) **[A3]**. The electrochemical characterization was performed on platinum foils. For other characterization experiments, the Pt electrodes were obtained by sputter-coating (Quorum Q150R ES, 60 mA) on glass slides **[A1, A4, A5, A6]** or polyester cover slips (Thermanox™) **[A2, A5, A7]**.

3.2. Electrochemical functionalization

Conducting polymer coatings, based on poly(3,4-ethylenedioxythiophene) (PEDOT) and/or poly(3,4-ethylenedioxypyrrole (PEDOP), on Pt electrodes were obtained by electrochemical polymerization of a corresponding monomer (10 mM), either 3,4-ethylenedioxythiophene (EDOT) or 3,4-ethylenedioxypyrrole (EDOP) in the presence of 0.1 M electrolyte (sodium poly(4-styrene sulfonate), NaPSS; lithium perchlorate, $LiClO_4$; sodium p-toluene sulfonate, pTS; tetrabutylammonium hexafluorophosphate, Bu_4NPF_6) in water **[A1, A4]** or acetonitrile (ACN) **[A1],** by a potentiodynamic method (cyclic voltammetry, CV) in a three-electrode system consisting of a Pt plate counter electrode and a Ag/AgCl (3 M KCl) reference electrode. Potential range was optimized for each monomer/electrolyte system separately.

Electrochemical grafting of diazonium salts was realized from a 3 mM solution of a single diazonium salt or a mixture of two diazonium salts **[A5, A6]** by CV in a three-electrode setup in the presence of 0.1 M tetrabutylammonium tetrafluoroborate (Bu_4NBF_4)/ACN solution. Potential range was optimized separately for each diazonium salt (4-nitrobenzenediazonium tetrafluoroborate (D-NO_2), 4-methoxydiazonium tetrafluoroborate (D-OCH_3), and 3,5-dichlorophenyldiazonium tetrafluoroborate (D-Cl_2)) and their binary mixtures (D-NO_2+D-OCH_3, D-OCH_3+D-Cl_2, D-NO_2+D-Cl_2).

3.3. Non-electrochemical coating strategies

Pt and diazonium-modified Pt surfaces were coated by drop-casting 50-100 µl of 1.5-4% poly(3,4-ethylenedioxythophene):poly(4-styrene sulfonate) (PEDOT:PSS) water dispersion **[A5]**. The electrodes were placed for 30 min on a heating plate (60 °C) to facilitate water evaporation.

3.4. Electrochemical characterization

The electrochemical studies were performed by means of a potentiostat equipped with a three-electrode system mentioned earlier. Cyclic voltammograms were collected with a scan rate of 100 mV/s in 0.1 M of a corresponding electrolyte. Charge storage capacity (CSC, C/cm^2) was calculated by integration of the area under the CV curve **[A1, A4, A5]** with the use of the following equation:

$$CSC = \int_{t_1}^{t_2} J(t)dt \tag{1}$$

where t_1 is the beginning of CV cycle (s), t_2 is the end of CV cycle (s), and J denotes the current density (A/cm^2).

CV curves were also collected at scan rates between 5 and 200 mV/s, and were used to calculate areal and volumetric capacitance **[A3, A4]**, with the use of the following equation:

$$C_{CV} = \frac{\int_{t_1}^{t_2} I(t)dt}{\Delta V} \cdot \frac{1}{X} \tag{2}$$

where C_{CV} denotes capacitance (F/cm^2 or F/cm^3) and ΔV denotes potential range (V). The X can be represented by area (A, cm^2) or volume (V, cm^3) in order to provide the areal or volumetric capacitance.

In **[A6]** a redox mediator, 1 mM $K_3[Fe(CN)_6]$, was added to the electrolytic solution to determine the relative anodic peak current (I_{rel}) based on the measured anodic peak currents (I_{pa}) and calculated based on the following equation:

$$I_{rel} = \frac{I_{pa}\ of\ modified\ electrode}{I_{pa}\ of\ bare\ Pt\ electrode} \cdot 100\% \tag{3}$$

Galvanostatic charging/discharging was performed at current densities between 0.1 and 5.0 mA/cm^2, and the results were used to calculate the areal and volumetric capacitance, energy density, power density, and coulombic efficiency **[A3, A4]** according to the following equations:

$$C_{GCD} = \frac{I \cdot t}{\Delta V} \cdot \frac{1}{X} \tag{4}$$

$$E = \frac{1}{2} C_{GCD} \cdot \Delta V^2 \div 3.6 \tag{5}$$

$$P = \frac{E}{t_D} \tag{6}$$

$$\eta = \frac{t_D}{t_C} 100\% \tag{7}$$

C_{GCD} denotes areal or volumetric capacitance (F/cm^2 or F/cm^3), I denotes current (A), t denotes time (s), ΔV denotes discharging potential difference (V), E denotes energy density (W·h/cm^2 or W·h/cm^3), P denotes power density (W/cm^2 or W/ cm^3), t_D denotes discharging time (h), t_C denotes charging time (h), and η denotes coulombic efficiency.

Electrochemical impedance spectroscopy (EIS) measurements were performed over frequencies ranging from 100 mHz to 100 kHz, at a DC potential of –0.10 to 0.22 V (vs. Ag/AgCl) and an AC amplitude of 10-50 mV. The recorded spectra were fitted into an equivalent circuit by means of EIS Spectrum Analyser 1.0 software [25] with the use of a Powell algorithm **[A1, A4, A5, A6]**.

3.5. Surface characterization

Surface wettability was measured with a goniometer by placing a 1 µl drop of deionized water (T ≈ 20 °C), and the resulting contact angle was measured **[A2, A6]**. An optical profilometer was used to analyze the surface roughness by deriving an arithmetic mean height (S_a) parameter according to ISO 25178 **[A6]**. Scanning electron microscopy (SEM) (10 – 15 kV) coupled with energy dispersive X-ray spectroscopy (EDS) was used to image the surface morphology **[A1, A2, A4]** and analyze the elemental composition **[A4]**. SEM coupled with focused ion beam (FIB-SEM) with a Ga source was used to etch the polymer coatings in order to reveal their cross-sectional surface and thickness (FIB: 1 nA beam current, followed by a polishing cut at 175 pA; SEM: 15 kV) **[A4]**. Fourier transform infrared spectroscopy (FTIR) measurements in the range from 500 to 1800 cm^{-1} were used for the chemical composition analysis **[A4]**.

3.6. Stability

Stability of coatings was determined by subjecting them to ageing or ultrasonication in phosphate-buffered saline (PBS) and examining the resulting solution with the use of UV-vis spectrophotometry **[A5]**. Scratch tests were performed by scratching the coating surface with a Rockwell diamond cone under gradually increased loading from 0.03 to 3.00 N over the length of 3 mm **[A4, A5]**. Three critical loads were determined: Lc_1 (load at which the first plastic deformation of the polymer layer occurred), Lc_2 (load at which the first damage to the polymer layer occurred, e.g. deformed conformal microcracks appeared) and Lc_3 (load at which complete damage occurred breaking the polymer layer).

3.7. Cell culture studies

Model cell lines: normal human dermal fibroblasts (NHDF) **[A2]** and human neuroblastoma (SH-SY5Y) **[A6, A7]** were used to estimate the biocompatibility of investigated surfaces. Cell viability was determined after 48 h of culture by their metabolic activity towards 3-[4,5-dimethylthiazol-2-yl]-2,5-diphenyltetrazolium bromide (MTT) **[A2]** or Alamar Blue **[A6]**. MTT reduction to formazan crystals was detected spectrophotometrically with the use of a microplate reader at 570 nm. In turn, the relative concentration of the reduced form of Alamar Blue was revealed by its fluorescence intensity (excitation 560 nm, emission 590 nm). In **[A7],** cell attachment was analyzed based on the number of cells present on the investigated surfaces after 1 h of incubation and washing with PBS. The surfaces were imaged with the use of a light microscope.

4. Results and discussion

4.1. Bioelectronic interfaces based on conducting polymers (CPs)

4.1.1. The effect of doping ion on electrochemical and biological performance of CP-based coatings

Although conducting polymers, and particularly PEDOT, have been frequently used for the modification of bioelectronic devices, the versatility of their performance is derived from the possibility to modulate their physicochemical characteristics through the judicious selection of polymerization conditions, including polymerization method – either chemical or electrochemical, and the choice of solvent and doping ions.

Accordingly, in **[A1]** I decided to investigate the effect of the selection of dopants (NaPSS, $LiClO_4$ and Bu_4NPF_6) on the polymerization potential, efficiency, and electrochemical properties of PEDOT-based conducting coatings. I optimized the polymerization potential range for each system separately, starting at -0.8 V (vs. Ag/AgCl) and adjusting the anodic limits (**Figure 1A-C**), in an effort to produce highly conducting films with improved capacitance – parameters that are crucial for biomedical applications of bioelectrode coatings, especially for electrophysiological stimulation [26]. The best electrical performance was observed for PEDOT/PF_6, which was formed with the use of an oxidation potential of 1.8 V in a Bu_4NPF_6/ACN system, while 1.2 V was optimal for both $LiClO_4/H_2O$ (PEDOT/ClO_4) and NaPSS/H_2O (PEDOT/PSS). The optimized polymerization curves are presented in **Figure 1D-F**. My results confirmed that conducting polymer films formed in organic solvents exhibited higher conductivity than those in aqueous solutions, likely due to greater conjugation length and improved electrode contact [27–29].

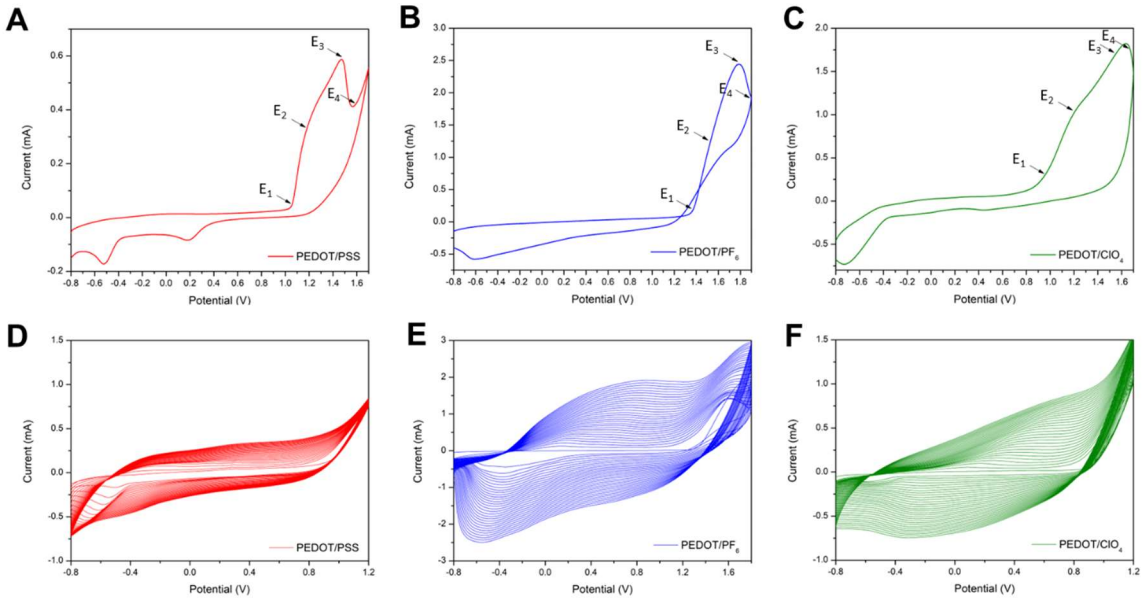

Figure 1. Optimization of electrochemical polymerization conditions for each doping system (PEDOT/PSS, PEDOT/PF_6, and PEDOT/ClO_4). CV curves show the selection of oxidative potentials based on the position of a polymerization peak, i.e. the onset potential (E_1), the half-peak potential (E_2), the peak potential (E_3), and the overoxidation potential (E_4), marked by arrows (A–C). CV curves showing the electropolymerization of EDOT under optimized conditions (D–F); 100 mV/s scan rate, 10 mM EDOT, 0.1 M corresponding electrolyte, 30 cycles.

In my research, I confirmed that polymerization conditions, including potential range, solvent, and doping ion, significantly impact the surface morphology of PEDOT. PEDOT/PF_6 exhibited a highly porous, sponge-like structure with micro- and nano-sized pores (**Figure 2A**), while PEDOT/ClO_4 had a more compact, grainy morphology (**Figure 2B**). PEDOT/PSS, however, showed a nonuniform surface with cavities and poor durability, undergoing visible degradation under electron probe exposure (**Figure 2C**). My findings align with previous studies, indicating that smaller dopant ions, such as PF_6^- and ClO_4^-, promote a more porous structure [30], whereas larger polymeric dopants like PSS^- result in a denser morphology. The influence of solvent was also significant, with water potentially hindering polymer formation through hydrogen bonding [31].

It is well known that surface morphology plays a crucial role in cellular adhesion. While rough surfaces can enhance cell attachment, the compatibility between cell size and surface features is also essential [32]. The cavities formed within the distinct polymer structures could offer better integration with axonal connections than a completely flat platinum surface. Based on the differences in surface morphology between PEDOT/PSS, PEDOT/PF_6, and PEDOT/ClO_4, I hypothesized that these surfaces should also interact differently when in contact with cells, which was further verified by the *in vitro* experiments with rat neuroblastoma cells (as described later in the text).

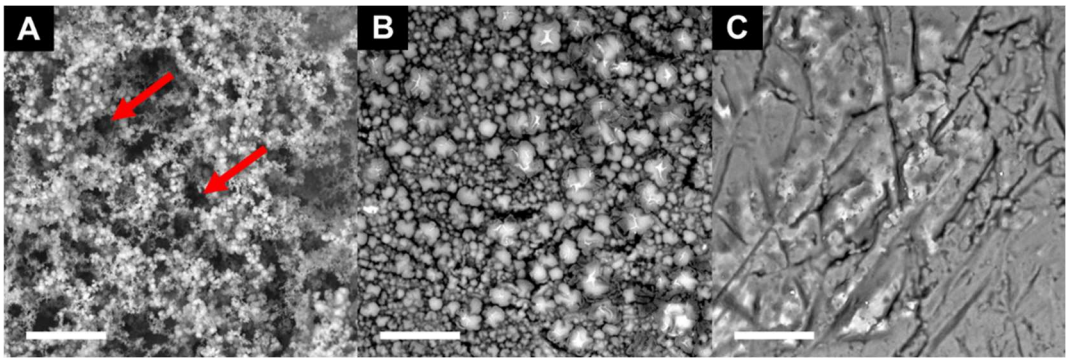

Figure 2. SEM surface images of PEDOT/PF_6 (A), PEDOT/ClO_4 (B) and PEDOT/PSS (C). The scale bar represents 30 µm and the red arrows indicate pores in the polymer structure.

In the next step, I compared the electrochemical properties of PEDOT matrices by analyzing their CV and EIS spectra collected in a monomer-free 0.1 M KCl solution (**Figure 3A**). The CV curves displayed a quasi-rectangular shape, indicating a capacitive character [33], with PEDOT/PF_6 showing the most developed profile, followed by PEDOT/ClO_4 and PEDOT/PSS. All three significantly outperformed the bare platinum electrode. Charge storage capacity (CSC), an important parameter for bioelectronic applications [34], was the highest for PEDOT/PF_6 (80.1 ± 6.3 mC/cm²), followed by PEDOT/ClO_4 (36.6 ± 1.8 mC/cm²) and PEDOT/PSS (18.4 ± 1.3 mC/cm²) (**Figure 3B**). The highest CSC of PEDOT/PF_6 was attributed to its highly porous structure, which increases the effective surface area for charge transfer. Impedance analysis (**Figure 3C**) revealed similar values of |Z| at 1 kHz for all PEDOT films, with PEDOT/PF_6 exhibiting the lowest impedance (113.8 ± 0.5 **Ω**).

To further assess the electrochemical behavior, I conducted an equivalent circuit analysis using EIS data. After multiple attempts, I decided that the most suitable circuit model to effectively describe all processes contributing to the impedance of PEDOT-based coatings would be the modified Randles circuit, previously proposed by Danielsson et al. [35] and later used by Kim et al. [36]. This model consists of a solution resistance (R_s), coupled with a double layer capacitance (C_{dl}) in parallel to a charge transfer resistance (R_{ct}), followed in series by a Warburg impedance element (Z_D) and a polymer bulk redox capacitance (C_d) (**Figure 3C-inset**). The inclusion of C_d was necessary to account for the phase angle shift from 45° to 90° observed at lower frequencies (**Figure 3D**). This model effectively described PEDOT behavior, which was confirmed by a high goodness of fit ($\chi^2 < 0.001$). The analysis confirmed that PEDOT/PF_6 had the highest capacitance (47.6 ± 7.1 mF/cm²), significantly exceeding that of PEDOT/ClO_4 (15.0 ± 0.8 mF/cm²) and PEDOT/PSS (7.0 ± 0.7 mF/cm²). While charge transfer resistance values remained similar across all PEDOT coatings, the capacitance differences highlighted the strong influence of the polymer morphology effect.

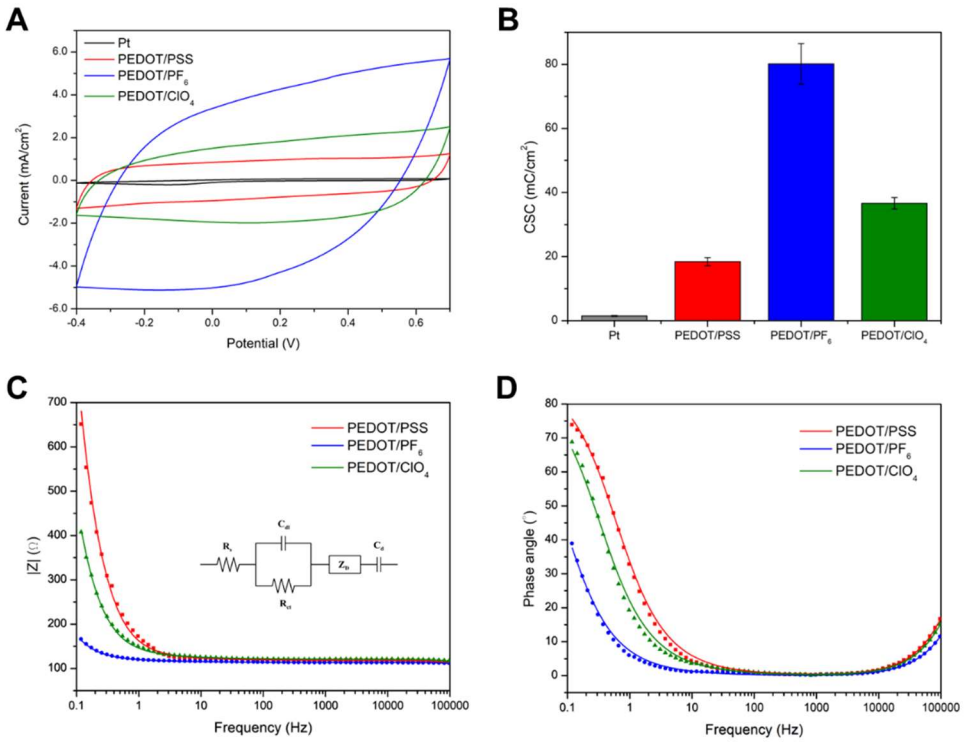

Figure 3. Electrochemical properties of Pt and PEDOT-based coatings. Cyclic voltammetry measured at 100 mV/s in 0.1 M KCl (A). Charge storage capacity obtained by integration of the CV data (B). Electrochemical impedance spectra measured at a DC potential of 0 V and an AC of 10 mV. The results are presented in the form of Bode plots with a modulus of impedance (C) and a phase angle (D) as a function of frequency. The equivalent circuit presented as an inset in (C) consists of a solution resistance (R_S), coupled with double layer capacitance (C_{dl}) in parallel to charge transfer resistance (R_{ct}) in series to Warburg impedance element (Z_D) and bulk polymer capacitance (C_d). The experimental data are presented in the form of points, whereas the fitted spectra are presented as continuous lines.

As complimentary experiments conducted by other investigators from our group, biocompatibility analysis was performed through viability, cell cycle, apoptosis and morphometric analysis with use of a rat neuroblastoma cell line (B35). Viability assay results showed PEDOT/ClO_4 as the most biocompatible (89% viability), slightly better than Pt (85%), while PEDOT/PF_6 (69%) was at the biocompatibility "threshold", and PEDOT/PSS (48%) should be treated as non-biocompatible. Cell cycle and apoptosis analysis confirmed that PEDOT/ClO_4 and Pt promoted proliferation, whereas PEDOT/PSS induced the highest cell death (29% sub-G_1 phase). Apoptosis assays revealed that PEDOT/PF_6 caused increased apoptotic death (31%), likely due to ACN traces, while PEDOT/PSS and Pt led to more necrotic cell loss. SEM imaging showed that PEDOT/ClO_4 facilitated axon branching, and the porous structure of PEDOT/PF_6 further enhanced cell integration. The surface of smoother PEDOT/PSS hindered attachment, while Pt provided adhesion but lacked complex cell-polymer interactions.

Overall, this study highlights the importance of dopant selection as the primary strategy in tailoring PEDOT's electrochemical and biological properties for bioelectronic applications. In particular,

PEDOT/PF_6 demonstrated exceptional charge storage capabilities, while PEDOT/ClO_4 showed superior biocompatibility, both surpassing the widely used PEDOT/PSS.

4.1.2. The effect of metal particles on biological performance of CP-based coatings

Modifying polymer surfaces with silver particles is a well-established method for imparting antibacterial properties to conducting polymers [37,38]. Toxicity of silver (nano)structures to bacteria and other cells is mostly mediated by silver ions release; therefore, it also depends on their morphology and concentration. Silver ions can be responsible for reactive oxygen species generation, enzyme inhibition, cell membranes disruption and induction of DNA damage, which are the proposed mechanisms of antimicrobial activity [39]. In contrast, gold has been one of the preferred materials for neural interface fabrication because of its excellent electrical conductivity, plasmonic characteristics, and high biocompatibility [40].

In the following approach to modulate the properties of PEDOT, the deposition of Au and Ag was used to potentially reduce the risk of infection after implantation **[A2]**. A PEDOT coating, synthesized in the presence of PBS solution, was modified by additional electrochemical deposition of Au and Ag particles from their ionic forms present in the solution (experimental details described in the Materials and methods section of **[A2]**).

Metal particle-modified PEDOT coatings were characterized with improved electrochemical properties, such as high charge storage capacity and decrease in impedance. Particularly, the CSC of PEDOT-Au and PEDOT-Au/Ag was improved by a factor of 3 (measured at 100 mV/s) over pristine PEDOT. The highest surface roughness (S_a) was obtained by introduction of Ag particles on PEDOT (0.241 ± 0.051 μm, when compared to 0.199 ± 0.013 μm for unmodified PEDOT). The S_a of gold-containing coatings were decreased to the values of 0.118 ± 0.002 μm and 0.128 ± 0.004 μm for PEDOT-Au and PEDOT-Au/Ag, respectively. The water contact angle was positively influenced by introduction of metal particles, resulting in surface wettability values ranging from ~47 to 60 °.

The antibacterial effect was evaluated by culturing *E. coli* on the PEDOT-based surfaces and measured with LIVE/DEAD assay and percentage of surface coverage. It was revealed that bacterial viability was highest on the surfaces of unmodified Pt (89 ± 1%) and PEDOT (85 ± 3%), while the presence of Ag significantly reduced the percentage of live bacteria (58 ± 4% for PEDOT-Ag and 57 ± 3% for PEDOT-Au/Ag). PEDOT-Au also decreased bacterial viability (68 ± 3%), though less effectively than Ag-containing surfaces. However, the most pronounced effect of metal particles was visible by reduction of bacterial coverage, which was the lowest for PEDOT-Au/Ag (1.1 ± 0.2 %).

In this work, I used my expertise in the characterization of cell-material interactions by performing mammalian cell culture studies and using an MTT assay to evaluate the cytotoxicity of coating strategies on normal human dermal fibroblasts (NHDF) (**Figure 4**). PEDOT significantly improved cell viability (140 ± 12%) compared to a Pt electrode control. However, adding Ag particles reduced biocompatibility, leaving only 34 ± 3% of viable cells. Au particles helped maintaining high cell viability (99 ± 8%) while mitigating Ag toxicity, resulting in 72 ± 5% viability for PEDOT-Au/Ag. Since mammalian and bacterial cells compete in a "race to surface" [41], selective toxicity is crucial for promoting tissue integration while preventing infection. Ag particles, lacking selectivity, were cytotoxic to both bacterial and mammalian cells, which is consistent with previous studies [42,43]. However, introducing Au particles before Ag deposition (PEDOT-Au/Ag) doubled NHDF viability while maintaining antibacterial efficacy. This may be attributed to Au's nanoporous-like topographical effects, influencing cell attachment and spreading via mechanotransduction [44]. Additionally, Au particles are known to reduce reactive oxygen and nitrite species [45] and production of inflammatory cytokines [46], further minimizing Ag-induced cytotoxicity. This highlights the balancing role of Au in preserving biocompatibility while retaining antibacterial properties.

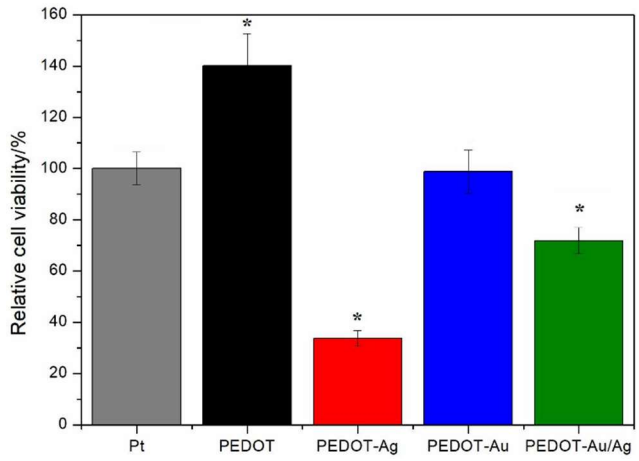

*Figure 4. Viability of NHDF cultured on Pt and PEDOT-based coatings after 48 h, based on MTT assay; *p<0.05.*

This research confirmed that by the deposition of Ag particles on the surface of PEDOT pre-modified with a layer of Au particles, it is possible to decrease the toxicity of Ag particles towards mammalian cells while preventing bacterial colonization. Additionally, the material's electroactive and capacitive properties make it suitable for various electroceutical applications. In this way, our study provides another instructive insight into the design of multifunctional coatings applicable in bioelectronic devices.

The concept of applying PEDOT decorated with metal particles as a bacteriostatic coating is a patent registered in the Patent Office of the Republic of Poland under the title *Conductive polymer coating, method of its preparation and application*; patent no. **PL246706**.

The main results derived from the studies I performed and described in this chapter underline the versatility of electrochemically deposited PEDOT-based coatings and the possibility of modulating relevant properties by the choice of solvent/dopant system or by inclusion of noble metal particles. It was highlighted how the choice of dopant – specifically ClO_4^- and PF_6^- – can significantly enhance the electrochemical performance, surface topography and biocompatibility of PEDOT films compared to the conventional PSS^- counterion. As a complementary strategy, the inclusion of Au and Ag particles into PEDOT resulted in the formation of a multifunctional coating with strong antibacterial properties and reduced cytotoxicity. These studies revealed the potential of carefully engineered PEDOT-based materials to meet the complex requirements of bioelectronics and electroceuticals, offering valuable insights into the design of multifunctional, biocompatible, and electroactive materials.

4.2. Conducting polymers as bio-supercapacitors

4.2.1. Supercapacitive properties of PEDOT:Nafion

Although conducting polymers are known as excellent neural interface materials, their application is not limited to neural electrode coatings. Due to their capacitive behavior, CP may also serve as efficient supercapacitors, as proved by numerous previous studies [47–50]. The combination of capacitive properties and biocompatibility suggests that CPs may be considered as implantable supercapacitors, potentially applicable for powering implantable devices, such as pacemakers, deep brain stimulators and cochlear implants [51,52].

Biocompatible supercapacitors have emerged as a key technology for the next generation of implantable and wearable bioelectronic devices, offering fast charge/discharge rates, long-term operational stability, and safe integration with biological systems [53]. Their development addresses the growing need for reliable, miniaturized, and non-toxic energy storage solutions in medical and health-monitoring applications. This aligns with broader global trends, as society moves away from fossil fuels and toward diverse, renewable energy sources [54]. In this evolving energy landscape, the demand for efficient, sustainable, and application-specific energy storage is becoming increasingly urgent. Biocompatible supercapacitors not only meet the unique requirements of bioelectronics but also contribute to the broader pursuit of innovative energy systems tailored for both environmental sustainability and personalized medicine [51,55].

Supercapacitors, next to batteries and fuel cells, are energy storage devices offering significant advantages, providing high power density and unparalleled fast charging and discharging, while maintain long cycling lifetime [55,56]. Depending on the charge storage mechanism, supercapacitors can be divided into electrical double layer capacitors and pseudocapacitors, which utilize electrostatic interactions or redox reactions, respectively [57]. In the latter group, the materials undergoing redox processes include metal oxides and CPs. Nonetheless, metal oxides, compared to CPs, are rather unfavorable due to high costs, toxicity, low processability and capacitance [58].

During my PhD I had the opportunity to take part in a collaboration with the researchers from the University of Ferrara in Italy led by Prof. Stefano Carli, aiming to utilize PEDOT modified with Nafion as a supercapacitor, potentially applicable to support the performance of bioelectronic devices. Among commonly studied conducting polymers for pseudocapacitor electrodes, PEDOT:PSS stands out due to its stability, water-based processability, affordability, and widespread use in organic electronics [59]. Though its conductivity is rather low (0.1–1 S cm^{-1}) [60], it can be significantly enhanced through secondary doping with polar solvents like dimethyl sulfoxide (DMSO) or ethylene glycol (EG). This treatment induces phase separation between conductive PEDOT and insulating PSS, improving carrier mobility and density [60,61]. Nafion is a copolymer

based on tetrafluoroethylene hydrophobic backbone, containing highly hydrophilic sulfonate groups [62]. Recently, the group of prof. Carli has developed and studied the possibility of replacing PSS by Nafion as an alternative polyanionic dopant [63]. Consequently, PEDOT:Nafion has been successfully synthesized as a stable water-based dispersion. It has been shown that PEDOT doped with Nafion instead of PSS is more conductive [63], and is characterized with improved stability [64] and adhesion to substrates [63]. Moreover, *in vitro* studies have proven its biocompatibility towards primary rat fibroblasts [65], making it a promising alternative as a neuroelectronic coating or as a supercapacitor material used in biomedical devices that require an internal power source [66].

Within this project, I was involved with testing the PEDOT:Nafion coatings developed in Prof. Carli's group in terms of their potential to be utilized in supercapacitor devices (**Figure 5**). I learned how to utilize electrochemical methods to test and quantify the capacitive properties of materials. As a result, my next publication **[A3]** explores charge storage properties of the pristine PEDOT:Nafion and solvent-treated coatings, either by EG or DMSO. In particular, PEDOT:Nafion treated with DMSO reached the areal capacitance of 22.2 ± 0.8 mF/cm^2 at 10 mV/s, and EG-treated PEDOT:Nafion exhibited low charge transfer resistance of 379 ± 19 Ω, being the result of a more effective ion diffusion inside the conductive film. Due to increased charge carrier density, DMSO-treated coating exhibited an excellent volumetric capacitance of 74.2 ± 4.2 F/cm^3, with a Coulombic efficiency of 99% and an energy density of 23.1 ± 1.5 mWh/cm^3 at a power density of 0.5 W/cm^3. A proof-of-concept symmetric supercapacitor based on PEDOT:Nafion exhibited a specific capacitance of approximately 15.7 F/g and notable long-term stability, indicating PEDOT:Nafion as a promising material for energy storage applications. Additionally, the fact that PEDOT:Nafion is biocompatible gives the possibility of using it as an implantable supercapacitor, which is the concept currently under investigation in our research groups.

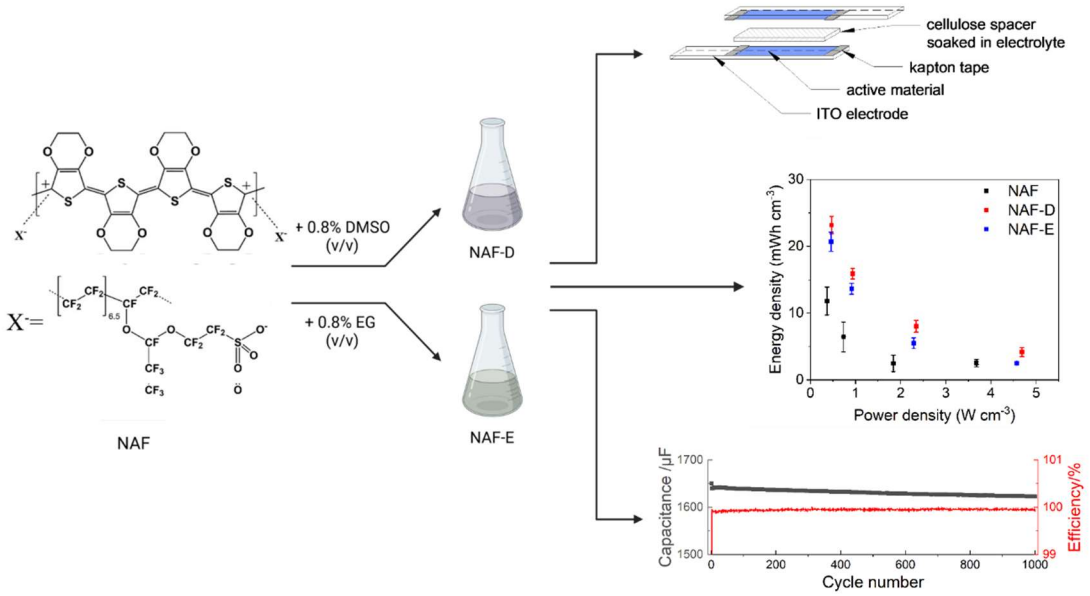

*Figure 5. Scheme representing the main concept of PEDOT:Nafion-based supercapacitor, described in **[A3]**.*

4.2.2. Bilayer supercapacitors based on PEDOT and PEDOP

The cooperation with Prof. Stefano Carli inspired me to further work in the field of implantable supercapacitors, resulting in the design and extensive characterization of another conducting polymer-based material. Based on my experience working with PEDOT and the vast expertise of my research group in developing PEDOP formulations, I decided to combine the two polymers into a superior material. Being a structural analogue to PEDOT, PEDOP shares similar advantages, including tunable physicochemical properties [67,68] and confirmed biocompatibility [69]. However, unlike EDOT, EDOP has a lower oxidation potential and is water-processable, which allows for more efficient electropolymerization in aqueous solutions [70]. Both polymers can be synthesized via electrochemical or chemical methods, allowing morphology optimization for better performance, as mentioned in the previous chapter. Their strong redox activity and the possibility of nanostructured film formation make them ideal candidates for supercapacitor electrodes. Additionally, the excellent biocompatibility of PEDOP, which was also proven in our group [69–71], enables its application for bio-integrated energy storage, including implantable medical devices and biosensors.

In **[A4],** PEDOT and PEDOP were electrochemically polymerized on Pt electrodes using cyclic voltammetry, with optimized polymerization potentials of 1.3 V (vs. Ag/AgCl) for EDOT, and 0.8 V (vs. Ag/AgCl) for EDOP (**Figure 6A,B**). Due to the large difference in polymerization potentials (~500 mV), simultaneous copolymerization was unsuccessful, as PEDOP overoxidation hindered EDOT oxidation. Instead, a step-by-step approach was used, depositing each monomer with 15 CV cycles. When EDOT was deposited first, PEDOP polymerized effectively, but reversing the order

led to PEDOP overoxidation, impairing the overall conductivity (**Figure 6C-D**). These findings confirm that sequential deposition, starting with EDOT, is the optimal strategy.

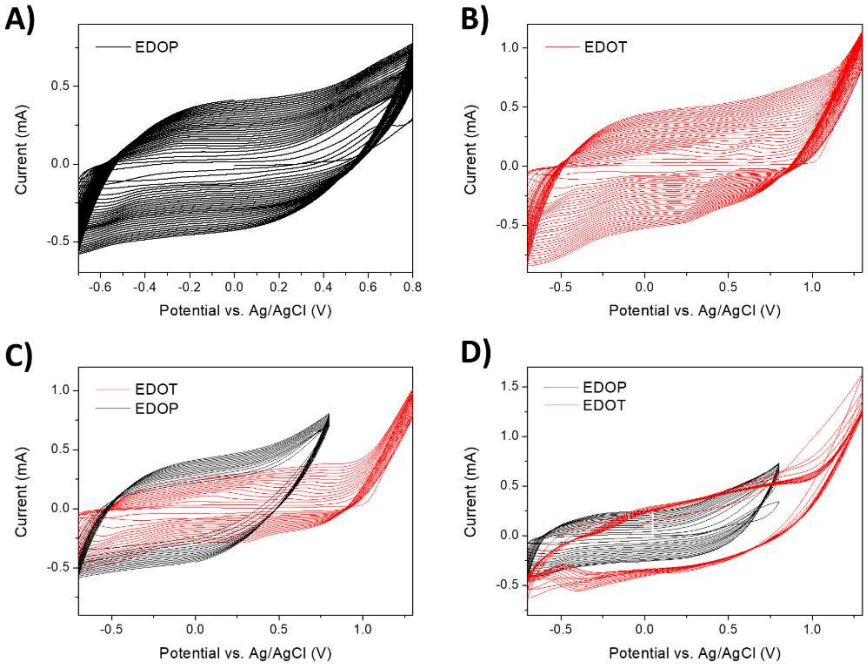

Figure 6. Electrochemical polymerization by cyclic voltammetry at a scan rate of 100 mV/s in 0.1 M pTS/H_2O and 10 mM of a corresponding monomer, for a total of 30 cycles. CV curves measured during polymerization of EDOP (A), EDOT (B), EDOP on PEDOT (C), and EDOT on PEDOP (D).

FTIR spectroscopy was used to confirm the chemical structures of PEDOT and PEDOP, with characteristic bands identified for both polymers (**Figure 7A**). The FTIR spectrum of PEDOT/PEDOP was dominated by PEDOP signals, indicating uniform coating over PEDOT, whereas PEDOP/PEDOT showed signals for both polymers, with evidence of PEDOP overoxidation. EDS analysis further verified the chemical composition, detecting carbon, oxygen, sulfur, and nitrogen (**Figure 7B-F**). Nitrogen presence confirmed effective PEDOP coating in PEDOT/PEDOP, while incomplete PEDOT coverage in PEDOP/PEDOT was observed. Additionally, sulfur distribution in PEDOT/PEDOP was non-uniform, suggesting some PEDOT exposure, though not strongly detected by FTIR.

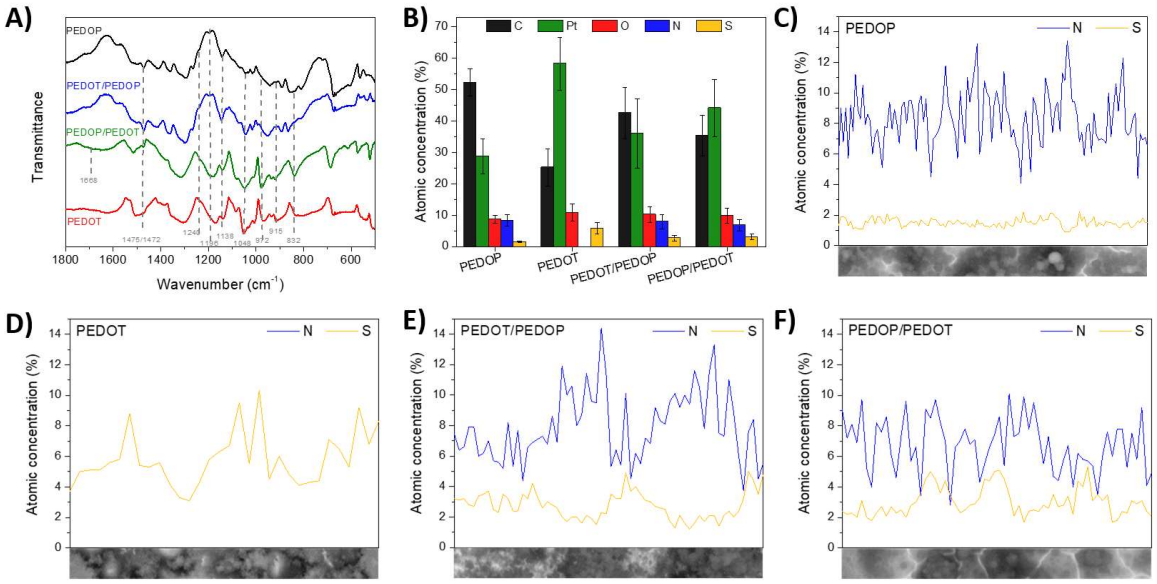

Figure 7. Spectroscopic analysis of polymer coatings. FTIR spectra with characteristic bands for PEDOT (1472 cm^{-1} – C═C, 972, 915, and 832 cm^{-1} – C─S─C) and PEDOP (1475 cm^{-1} – C═C, 1240 cm^{-1} and 1196 cm^{-1} – C─N, 1138 and 1048 cm^{-1} – C─O─C) (A). EDS results presenting surface composition by atomic concentration of elements (B) and line scans presenting nitrogen and sulfur composition (C-F).

The enhanced electrochemical properties of PEDOT/PEDOP were examined using atomic force microscopy (AFM) and SEM (**Figure 8A**), comparing nano-scale ($S_{a,AFM}$) and micro-scale ($S_{a,SEM}$) roughness (**Table 1**). PEDOP featured fused spherical structures, while PEDOT had a more developed, porous surface with intersecting cavities. PEDOT/PEDOP exhibited the highest roughness ($S_{a,SEM}$ of 1.59 ± 0.20 µm), with smaller PEDOP-like round structures increasing surface area available for ion interaction and charge storage [72]. In contrast, PEDOP/PEDOT showed visible microcracks, indicating the damaging effects of PEDOP overoxidation.

Thanks to my internship at the University of California, Irvine, I had a chance to join the group of Prof. Zuzanna Siwy and use the focused ion beam (FIB) etching to analyze the internal microstructure of investigated materials. FIB-SEM allowed to reveal the polymers' cross-sections and thickness (**Figure 8B, Table 1**). PEDOP was characterized with the lowest thickness (1.00 ± 0.13 µm) and a compact structure, while PEDOT was over four times thicker (4.24 ± 1.39 µm) and highly porous throughout the bulk of the polymer. PEDOT/PEDOP had an intermediate thickness (2.19 ± 0.46 µm), with smaller, less frequent cavities, suggesting that EDOP polymerized within the PEDOT's porous structure. This led to an increase in the electroactive surface area, enhancing electrochemical capacity. Their similar molecular structure ensured high compatibility, enabling a synergistic effect that facilitated electrolyte access.

To examine the potential stability in long-term applications, a scratch test was performed on the polymer coatings. Consequently, PEDOP was found to have the highest adhesion strength (1.89 ± 0.31 N), slightly outperforming PEDOT (1.53 ± 0.30 N). PEDOP on PEDOT improved adhesion

of the latter (1.70 ± 0.50 N) by reducing surface cavities and, therefore, increasing the electrode contact surface. However, PEDOP/PEDOT required the least force for complete coating damage due to its cracked surface. Despite these variations, differences in adhesion strength were not statistically significant due to high surface roughness and non-uniformity (**Table 1**).

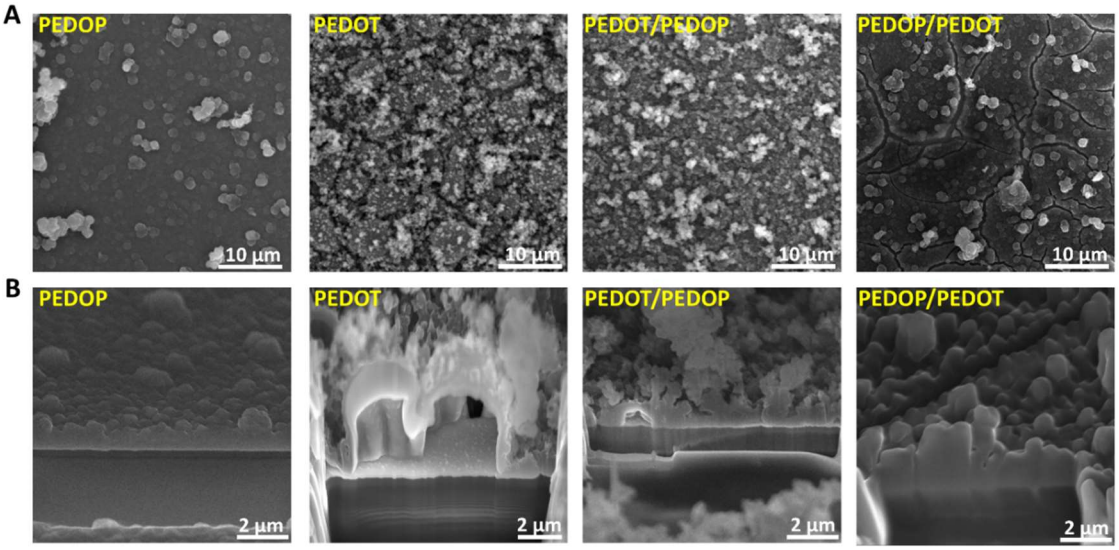

Figure 8. SEM surface (A) and cross-section images (B) of PEDOT, PEDOP, PEDOT/PEDOP and PEDOP/PEDOT films. The cross-section images were obtained after FIB etching.

Table 1. Physical properties determined by SEM, AFM and scratch test.

	PEDOP	PEDOT	PEDOT/PEDOP	PEDOP/PEDOT
Thickness, µm	1.00 ± 0.13	4.24 ± 1.39	2.19 ± 0.46	1.29 ± 0.28
Nano-scale roughness, $S_{a,AFM}$, nm	184.1 ± 4.9	318.0 ± 2.8	330.9 ± 4.7	276.3 ± 7.6
Micro-scale roughness, $S_{a,SEM}$, nm	960.8 ± 359.9	1223.3 ± 220.6	1592.0 ± 205.7	1042.4 ± 266.3
Adhesion strength, L_{C3}, N	1.89 ± 0.31	1.53 ± 0.30	1.70 ± 0.50	0.86 ± 0.65

EIS results (**Figure 9A-B**) showed that PEDOT/PEDOP exhibited the lowest impedance, particularly at low frequencies, indicating reduced ion diffusion resistance and higher capacitance. Equivalent circuit modeling confirmed that PEDOT/PEDOP had the lowest charge transfer resistance (25 ± 8 Ω), highest capacitance (4.38 ± 0.40 mF), and improved charge diffusion (25 ± 8 $\Omega/s^{1/2}$), highlighting the beneficial effect of PEDOP within PEDOT's 3D structure.

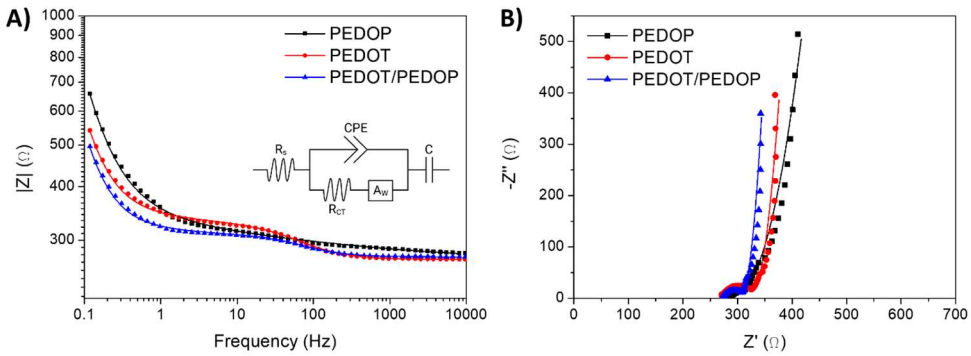

Figure 9. Electrochemical impedance spectroscopy results presented in the form of Bode (A) and Nyquist (B) plots. The equivalent circuit is presented as an inset (A). EIS measurements were performed in 0.1 M pTS/H_2O at a DC potential of 0 V (vs. Ag/AgCl) and an AC voltage amplitude of 10 mV. Experimental data is represented by separate points and the fitted spectra are shown as continuous lines.

To evaluate the effectiveness of PEDOT/PEDOP for supercapacitor applications, cyclic voltammetry and galvanostatic charge–discharge (GCD) analyses were conducted. CV curves were recorded at various scan rates to evaluate the areal and volumetric capacitance. The results showed a nearly linear increase in capacitance with lower scan rates, indicating better ion diffusion. PEDOT/PEDOP exhibited the highest areal capacitance (42.2 ± 2.8 mF/cm² at 5 mV/s), outperforming both PEDOP (32.5 ± 2.9 mF/cm²) and PEDOT (33.1 ± 6.8 mF/cm²) (**Figure 10A**). However, PEDOP had the highest volumetric capacitance (323.8 ± 28.5 F/cm³) due to its lower thickness (**Figure 10B**). Similarly, with the GCD testing method, PEDOT/PEDOP's superior areal capacitance was established (21.02 ± 1.97 mF/cm² at 0.1 mA/cm²) (**Figure 10C**), while due to its compactness, PEDOP had the highest volumetric capacitance (151.48 ± 6.91 mF/cm³) (**Figure 10D**). GCD data was also used to establish energy density versus power density relations (**Figure 10E-F**), which are frequently used for comparison of supercapacitor performance [73]. In terms of volumetric energy density, PEDOP reached the highest value (25.5 ± 1.2 mWh/cm³), outperforming both PEDOT/PEDOP (16.1 ± 1.5 mWh/cm³) and PEDOT (6.5 ± 0.7 mWh/cm³). In contrast, the highest areal energy density was reached for PEDOT/PEDOP (3.53 ± 0.33 μWh/cm^2 at 55 μW/cm^2).

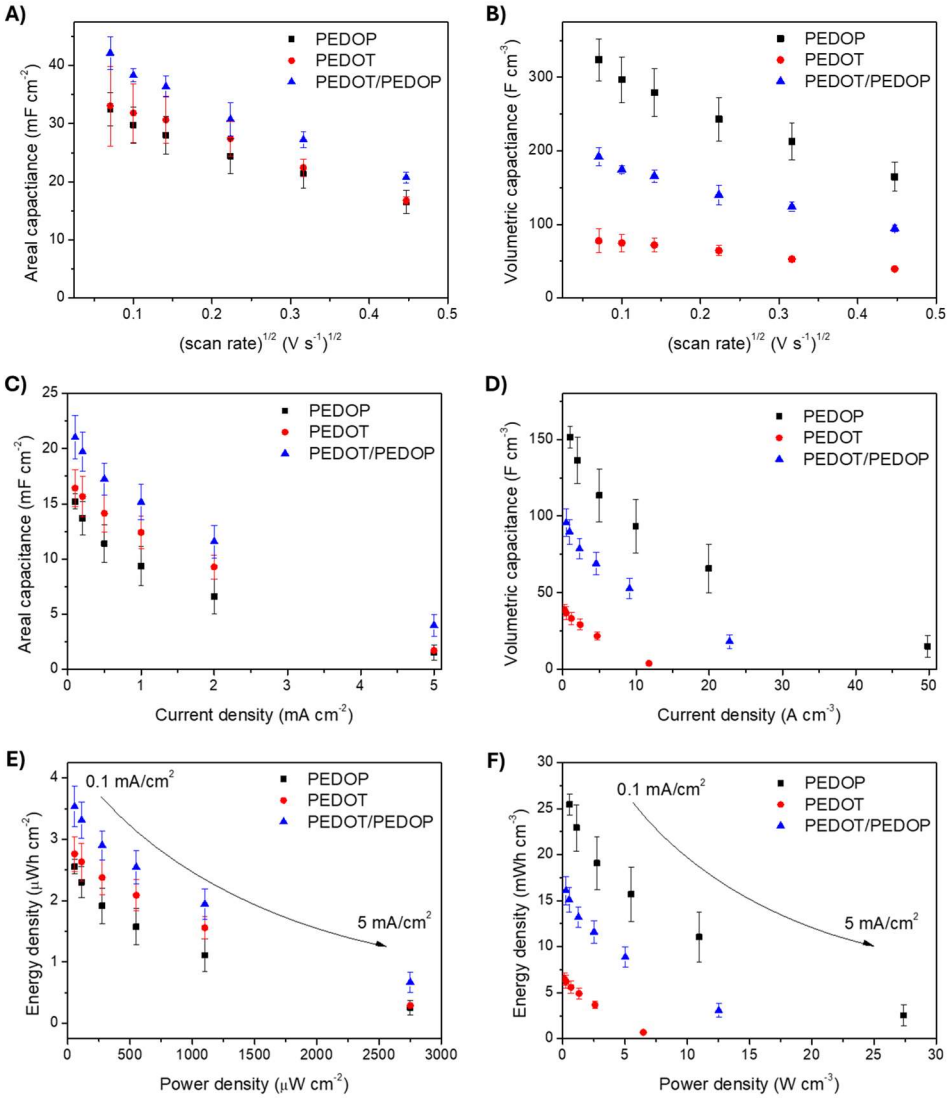

Figure 10. Capacitive properties of PEDOT, PEDOP and PEDOT/PEDOP coatings in respect to area (A, C, E) and volume (B, D, F). The data are based on CV (A, B) and GCD (C-F) measurements. All experiments were conducted in 0.1 M pTS/H_2O.

Conducting polymer coatings are particularly advantageous in forming thin layers, where their performance is more reliant on electrolyte penetration rather than volume scaling [74]. As thickness increases, performance can degrade due to hindered ion diffusion in larger volumes, leading to reduced stability and a higher risk of delamination [75]. Therefore, areal capacitance becomes a crucial property for evaluating the charge storage properties of these materials, as it is the most scalable. Additionally, the advantage of the PEDOT/PEDOP bilayer is that its capacitive properties are enhanced simply by adjusting the polymeric material's morphology through a layer-by-layer deposition approach, without needing any additional fillers. Finally, the cytocompatibility of both PEDOT and PEDOP, combined with the growing popularity of wearable and implantable bioelectronics, presents a promising opportunity for developing biocompatible charge storage elements based on these polymers.

The concept of applying PEDOT/PEDOP material as a capacitive coating was submitted as a patent application into the Patent Office of the Republic of Poland under the title *Layered polymer system, method of obtaining it and use for electrical energy storage*; registration no. **P.449856**.

In this chapter, the applicability of CP-based coatings was extended to a broader scope of applications by exploring their charge storage characteristics. Notably, solvent-treated PEDOT:Nafion films demonstrated excellent electrochemical properties, such as high capacitance, low charge transfer resistance, and long-term stability, outperforming the gold-standard PEDOT:PSS. Similarly, the PEDOT/PEDOP composite, synthesized through a layer-by-layer approach, surpassed the limitations of the individual homopolymers due to its optimized 3D architecture and efficient ion transport properties. Enhancing capacitive performance through molecular and morphological design demonstrates the versatility of these materials for energy storage applications. Moreover, their demonstrated biocompatibility, as discussed in the previous chapter and earlier studies, further expands their relevance to powering implantable bioelectronic systems.

4.3. Bioelectronic interfaces based on electrodeposited thin organic films

4.3.1. The problem of coating stability mitigated by diazonium monolayers deposition

As discussed in the previous chapters, CPs offer several advantages in bioelectronic applications, including compatibility with tissue, and improved electrochemical and surface properties. However, CP-coated devices often fail due to poor adhesion, cracking, and delamination of the polymer layer [76], leading to reduced lifespan, increased costs, and potential health risks of biomedical implants [77].

Various strategies to enhance CP adhesion, like substrate nanopatterning [78] and the modification of surfaces with pro-adhesive coatings based on self-assembled monolayers [79], are often complex or time-consuming. Electrografting of aryldiazonium salts offers a simpler, effective approach for creating adhesive monolayers on electrode surfaces [80,81]. For example, improved adhesion of electropolymerized PEDOT has been demonstrated on Pt/Ir, ITO, and gold electrodes pre-treated with various custom-synthesized diazonium salts [77,82,83]. However, these diazonium compounds are not commercially available and require complex synthesis. Moreover, the enhanced adhesion was shown for electropolymerized PEDOT, not PEDOT:PSS dispersions, which are more accessible and widely used in industry.

Poly(3,4-ethylenedioxythiophene):poly(4-styrene sulfonate) (PEDOT:PSS) is the most commercially successful conducting polymer, which popularity stems from processability, tunable conductivity, transparency to visible light, thermal stability, and biocompatibility [84]. In our approach, we developed a new surface pretreatment method that improved the adhesion of PEDOT:PSS to platinum electrodes, reduced charge transfer resistance, and enhanced coating capacitance **[A5]**. Our approach used a one-step electrochemical grafting process on Pt electrodes with commercially available diazonium salts (D-NO_2, D-OCH_3 and D-Cl_2). Subsequently, PEDOT:PSS was deposited on those surfaces by a drop-casting method, which led to the formation of more stable CP coatings (PEDOT/D-NO_2, PEDOT/D-OCH_3, and PEDOT/D-Cl_2) with favorable electrical properties. In this project, I was responsible for developing the methodology for electrochemical deposition and characterization while supervising the experiments performed by a bachelor student.

The electrochemical characterization of PEDOT:PSS drop-casted on Pt and diazonium-functionalized Pt surfaces was performed by CV and EIS. The results showed that surface treatment with diazonium salts led to more developed CV curves and higher CSC values. The CSC of all PEDOT samples increases with a decreasing scan rate (**Figure 11A**), due to the presence of internal active sites. Therefore, lower scan rates allow a better estimation of the electrode's capacitive properties [85]. At 10 mV/s, PEDOT:PSS deposited on modified electrodes achieved a CSC of 235 mC/cm², which is 35% higher than PEDOT:PSS deposited on unmodified Pt (175 mC/cm²). EIS

spectra shown as a Nyquist plot (**Figure 11B**) revealed similar electrical properties for all PEDOT:PSS-coated electrodes, indicating a consistent charge transfer mechanism. Consequently, a modified Randles circuit (**Figure 11B-inset**) was used to simulate all EIS data. This model includes a solution resistance (R_s) in series with a charge transfer resistance (R_{ct}) parallel to a double-layer capacitance (C_{dl}), and a constant phase element (Z) representing polymer capacitance, as previously used in **[A1]**. PEDOT:PSS on unmodified Pt showed the highest charge transfer resistance, R_{ct} (67.3 ± 1.6 Ω), and the lowest polymer capacitance, Z (6.7 ± 0.1 mF), as indicated by the largest semicircle in the Nyquist plot. Surface treatment with diazonium salts significantly reduced R_{ct} (15.0 ± 0.5 Ω for PEDOT/D-NO_2) and increased capacitance (up to 13.3 ± 0.8 mF for PEDOT/D-OCH_3), suggesting improved ion diffusion within the film.

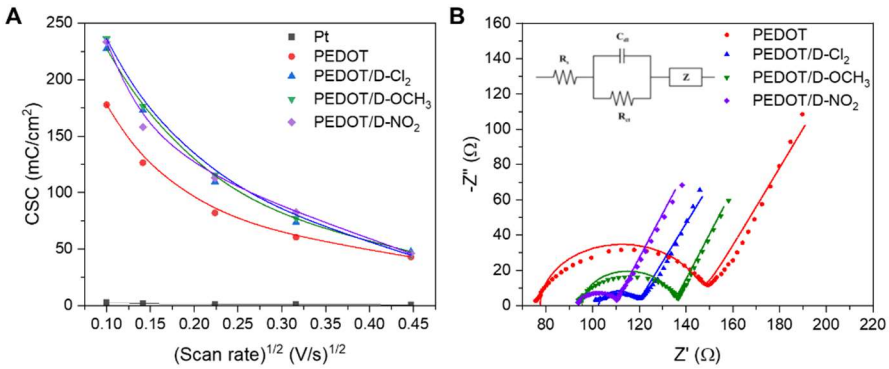

Figure 11. Electrochemical properties of Pt and PEDOT:PSS. Function of CSC and scan rate, based on CV measurements (A). Nyquist plot based on EIS measurements and an equivalent circuit shown as an inset (B). The experimental data is represented by points, whereas the continuous lines show the fitted spectrum. All measurements were conducted in PBS solution.

Stability of PEDOT:PSS on Pt electrodes was evaluated by exposing them to 30 days of ageing in PBS (AG), 3 minutes of ultrasound (US) treatment, or a scratch test. UV–vis spectra of PBS solutions after these treatments showed characteristic peaks for PEDOT (325 nm) and PSS (268 nm) [86,87]. For PEDOT-modified electrodes without aryl layers (**Figure 12A**), absorbance between 200–400 nm was similar for AG and US treatments. The increased peak at 268 nm after US treatment suggests coating degradation resulting in the partial dissolution of PSS, likely due to its higher hydrophilicity compared to PEDOT, which led to PEDOT:PSS dedoping. In contrast, ageing for 30 days resulted in both PSS and PEDOT being found in the PBS solution.

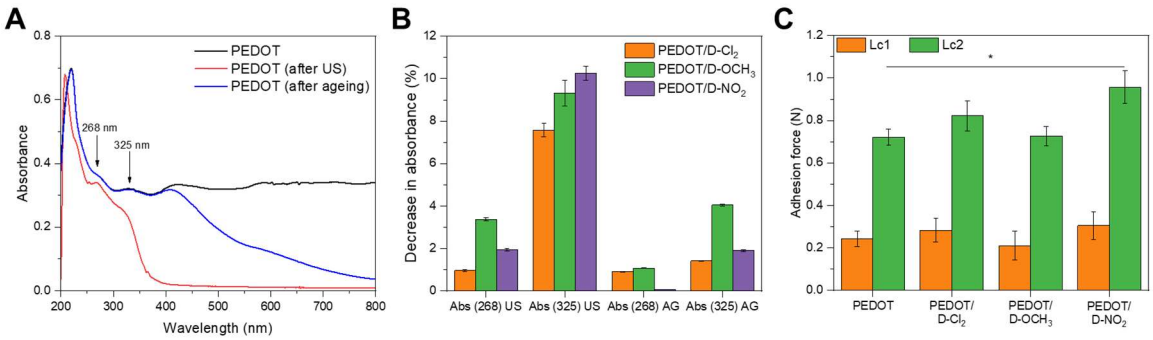

Figure 12. Stability of PEDOT:PSS on Pt electrodes. UV–vis spectra of a 0.02% PEDOT:PSS solution in PBS (black line), and a PBS solution after US treatment (red line) and AG (blue line) collected over non-pretreated PEDOT-coated electrodes (A). Decrease in the absorbance at characteristic wavelengths after AG and US treatment for pretreated Pt electrodes coated with PEDOT with respect to non-pretreated PEDOT-coated electrodes (B). Comparison of adhesion forces (L_{c1} – loading at which polymer layer was scratched, L_{c2} – loading at which polymer layer was fully damaged).

To assess the impact of electrode pretreatment with aryl layers on PEDOT:PSS coating stability, UV-vis spectra of PBS solutions after AG and US treatment of PEDOT/D-OCH_3, PEDOT/D-NO_2 and PEDOT/D-Cl_2 were compared to non-pretreated PEDOT electrodes. **Figure 12B** shows a decrease in absorbance for pretreated electrodes resulting from decreased concentration of PEDOT and PSS in the PBS solution. In turn, this indicates that electrografting improved PEDOT:PSS layer stability, making it less prone to delamination. Electrografting reduced the dissolution of PSS and PEDOT, with the strongest effects for D-NO_2 and D-OCH_3. Scratch test results (**Figure 12C**) confirmed that more force was required to damage PEDOT:PSS on electrodes electrografted with D-NO_2. The adhesion force for PEDOT/D-NO_2 was 0.96 ± 0.08 N, 33% higher than that of PEDOT on unmodified Pt (0.72 ± 0.04 N). This enhanced adhesion is likely due to improved physical interactions, such as hydrogen bonding or electrostatic interactions, between the polymer and functional groups on the pretreated surface [81].

This study demonstrated that surface modification with commercially available diazonium salts can improve the adhesion, charge transfer, and mechanical stability of PEDOT:PSS, a widely used conducting polymer in organic electronics. This can translate into improved performance of bioelectronic CP-based devices, increasing their safety and longevity.

The concept of applying diazonium salts as adhesion layers for PEDOT:PSS has been a subject of a patent application submitted into the Patent Office of the Republic of Poland under the title *Pro-adhesive organic coating and method of obtaining it*; registration no. **P.444426**. The patent was granted on 13.03.2025.

4.3.2. Diazonium salts for antibacterial coatings

To assess the influence of electrografting of diazonium salts on the properties relevant for bioelectronic interfaces, I decided to perform in-depth experiments on the thin organic layers themselves **[A6]**. I hypothesized that the different functional groups of diazonium salts used in electrografting of organic monolayers would yield electrode coatings with differing electrochemical and surface properties, such as wettability, cell adhesion, cell viability, and antibacterial activity. Furthermore, I proposed that mixed monolayers, derived from binary mixture of diazonium salts, could synergistically integrate the advantages of both components.

Consequently, I functionalized Pt electrodes by electrochemical grafting of D-NO_2, D-OCH_3, D-Cl_2, and their binary mixtures: D-NO_2+D-OCH_3, D-OCH_3+D-Cl_2, and D-NO_2+D-Cl_2. The optimized CVs (**Figure 13A-C**) present broad cathodic peaks corresponding to the reduction of diazonium cations to aryl radicals, accompanied by nitrogen release. The reduction potentials varied based on the electronic nature of the substituents [88], with D-NO_2 showing the most positive potential (0.27 V vs. Ag/AgCl) due to its electron-withdrawing nitro group, while D-OCH_3 had the most negative potential (−0.12 V vs. Ag/AgCl) due to its electron-donating methoxy group. D-NO_2 and D-Cl_2 exhibited similar reduction currents (~ −0.15 mA), suggesting a comparable deposition pathway, though D-NO_2 showed a larger peak area, indicating that deposition continued beyond monolayer formation. During the second CV cycle, reduction peaks for D-NO_2 and D-Cl_2 nearly disappeared. D-OCH_3 displayed a higher reduction current (−0.2 mA) and maintained a significant reactivity in further cycles, suggesting high affinity to multilayers formation and lower tendency to fully saturate the Pt surface [89].

The deposition conditions for mixed aryl layers were optimized by adjusting the potential range and salt concentration ratios to visualize both reduction peaks (**Figure 13D-F**). Interestingly, the presence of a mixture of diazonium salts was found to influence peak positions. When D-NO_2 and D-OCH_3 were combined, the reduction peak of D-OCH_3 shifted to a more negative potential (−0.35 V vs. Ag/AgCl), suggesting reduced deposition efficiency on D-NO_2-coated surfaces. In contrast, mixing D-OCH_3 with D-Cl_2 facilitated D-Cl_2 reduction, shifting its potential from 0.10 V to 0.27 V. The reduction potentials remained unchanged when D-NO_2 and D-Cl_2 were mixed.

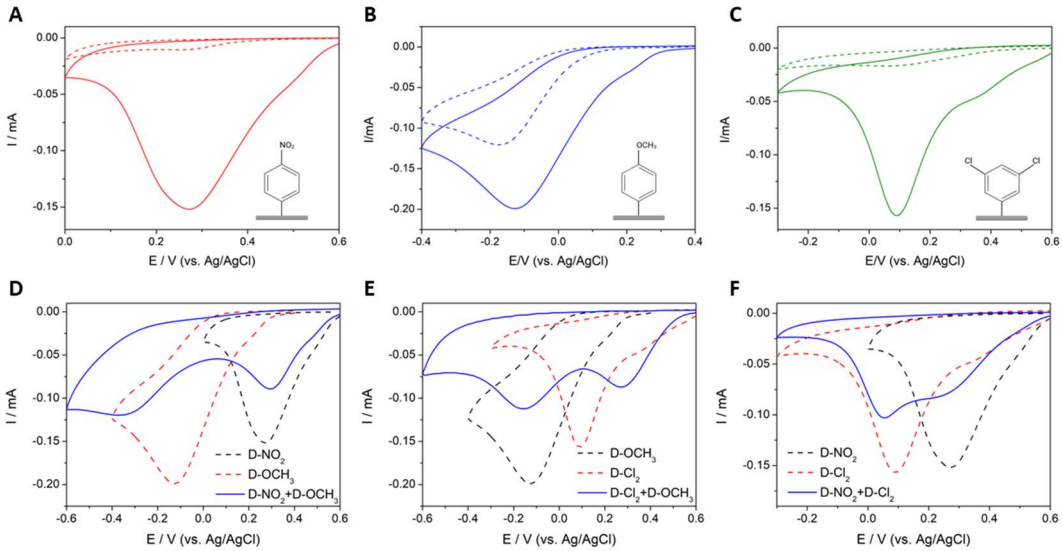

Figure 13. Electrografting of diazonium salts from solution containing a single salt type (A, B, C) and from binary mixtures of diazonium salts (D, E, F). In all experiments the total concentration of diazonium salt(s) remained at 3 mM and the supporting electrolyte was 0.1 M Bu_4NBF_4 in ACN.

Electrochemical methods were used to evaluate the electroactivity, conductivity, and capacitance of functionalized electrode surfaces in the presence of a redox mediator. The summary of electrochemical properties is presented in **Table 2**. CVs were collected to assess the blocking properties and compactness of the organic layers [81]. The D-Cl_2 layer showed the highest passivation, reducing the relative anodic peak current (I_{rel}) by 98.4 ± 0.8% compared to bare Pt, indicating a compact layer and increased charge transfer resistance (R_{ct}). D-OCH_3 had a lower passivation effect (81.9 ± 3.3% relative peak current) due to possible side reactions, while D-NO_2 showed moderate passivation (27.6 ± 9.8%). EIS spectra confirmed increased impedance and suggested two capacitive elements. EIS data were fitted to a modified Randles circuit [90], showing that diazonium modifications reduced electroactivity and increased R_{ct}, while maintaining comparable capacitance.

Table 2. Electrochemical properties derived from CV and EIS measurements in the presence of a redox mediator.

Pt functionalization	**Relative anodic peak current, I_{rel} (%)**	**R_{ct} (Ω)**
none	100	68 ± 20
D-NO_2	27.6 ± 9.8	853 ± 135
D-OCH_3	81.9 ± 3.3	320 ± 54
D-Cl_2	1.6 ± 0.8	12365 ± 1328
D-NO_2 + D-OCH_3 (1:3)	19.3 ± 2.2	622 ± 96
D-Cl_2 + D-OCH_3 (1:3)	8.7 ± 4.8	2387 ± 81
D-NO_2 + D-Cl_2 (1:7)	1.5 ± 1.1	6750 ± 1328

The measurements of surface wettability were used as a simple way to confirm successful electrode functionalization. Diazonium-based layers significantly increased the water contact angle of Pt electrodes, indicating enhanced hydrophobicity (**Figure 14A**). The D-Cl_2 layer had the highest contact angle (95 ± 3°), which was over five times greater than bare Pt (17 ± 5°). D-OCH_3 showed the lowest increase (50 ± 4°) due to its more hydrophilic nature. Mixed layers had contact angles averaging those of individual layers, suggesting a nearly equimolar surface composition. Roughness measurements (**Figure 14B**) showed less dramatic changes, with the greatest increase (2.5-fold) for the D-NO_2+D-Cl_2 mixture. The low roughness of modified surfaces compared to bare Pt indicated uniform and compact organic layers [91]. Mammalian cells generally prefer moderately rough (20–30 nm) and less hydrophilic surfaces (contact angle >65°) [92], while bacterial cells favor smoother surfaces (S_a <6 nm) [93]. Therefore, the noted differences between water contact angles and roughness of bare and modified Pt surfaces supported the hypothesis that the electrodeposition of diazonium salts and their binary mixtures could affect cell adhesion.

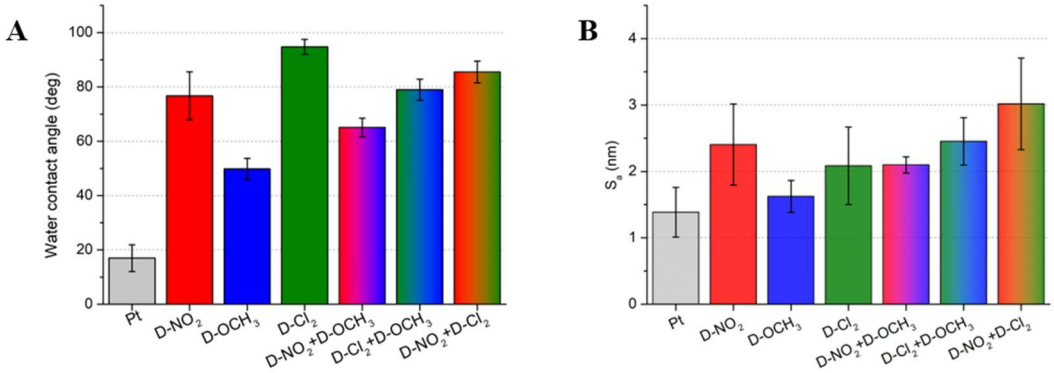

Figure 14. Surface properties. Water contact angle obtained by goniometer (A). Surface roughness measured with the use of an optical profilometer (B).

To verify biocompatibility of organic monolayers, SH-SY5Y human neuroblastoma cells were cultured on modified and unmodified Pt electrodes for 48 hours. The Alamar Blue assay, which was used to measure cell metabolic activity, showed cell viability above 88% for all samples (**Figure 15A**). According to ISO 10993-5:2009 [94], materials with over 70% cell viability are considered biocompatible. These results indicate that none of the coatings negatively affected cell adhesion or viability, suggesting that they are suitable as biocompatible coatings.

E. coli were cultured on modified and unmodified Pt surfaces for 48 hours. Diazonium-modified surfaces significantly reduced bacterial density, with D-Cl_2 and the D-NO_2+D-Cl_2 mixture showing the strongest effect (84% reduction) (**Figure 15B**). Other coatings (D-NO_2, D-OCH_3, and D-NO_2+D-OCH_3) also lowered bacterial presence by 45%−51%. Live/dead assay showed similar live-to-dead bacteria ratios on all surfaces. D-OCH_3 and D-NO_2+D-OCH_3 samples had more variability, likely due to non-uniform layer formation. The D-NO_2 coating slightly reduced live bacteria (from

76 ± 2% on Pt to 64 ± 2%), while other modified surfaces had higher viability than bare Pt, with D-Cl_2+D-OCH_3 showing the highest percentage of live cells (92 ± 3%). Notably, this surface also had the lowest bacterial coverage. Overall, diazonium-derived layers did not kill bacteria but effectively prevented their adhesion, which is key to reducing implant-associated infections. Reduced adhesion of *E. coli* correlated with lower surface wettability and increased nano-roughness, supporting previous findings that roughness can deter bacterial adhesion [93].

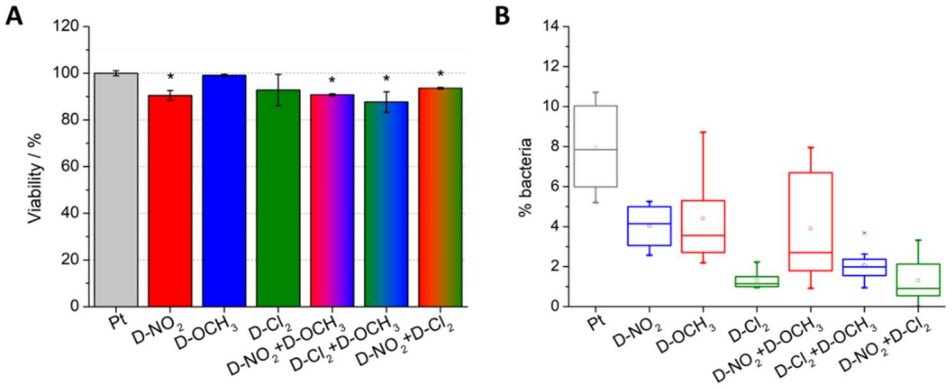

*Figure 15. Biological properties of Pt electrodes functionalized with organic monolayers. Viability of SH-SY5Y evaluated with Alamar Blue assay after 48 h of incubation (A); * p<0.01. Percentage of E. coli bacterial coverage presented in the form of a box plot (B); box limits indicate the data within the first and third quartiles, with the horizontal line representing the median value, square symbol represents the mean value, whiskers correspond to 1.5 of the interquartile range.*

Miniaturization is crucial in implantable medical devices, as smaller devices reduce tissue disruption [95]. In neuromodulation and neurorecording, smaller electrodes enable more precise control, such as activating or recording signals from individual cells [96], and allow for compact, complex electrode architectures [97]. Therefore, as part of my internship with Prof. Maria Asplund at the University of Freiburg, I was able to demonstrate that even micro-sized surfaces (d = 500 µm, **Figure 16A**) can be successfully modified with organic layers. Smaller surface areas resulted in more compact layers, particularly with D-Cl_2, where the typical redox peaks of $K_3[Fe(CN)_6]$ disappeared, and impedance increased. Binary mixtures also formed more compact layers, without any redox signals from the probe. D-OCH_3 on microelectrodes caused only a minimal increase in the impedance of Pt across the entire frequency range. While it was less effective in preventing bacterial adhesion compared to other diazonium formulations, it was the most promising for modifying electrode surfaces without significantly compromising electrochemical performance. Coating microelectrodes with modifications that blocked electron transfer, as shown by the disappearance of redox signals for the remaining coatings, can be used to reduce interference in implantable biosensors [98]. Electrochemical grafting of diazonium salts is also compatible with various conductive surfaces, including titanium [99], Co-Cr alloys [100], and stainless steel [101], making it a promising method for adding antibacterial properties to biomedical materials without

compromising biocompatibility. Additionally, electrodeposited diazonium salts offer an alternative to photolithography for micropatterning, simplifying the process, as proposed in **Figure 16B**.

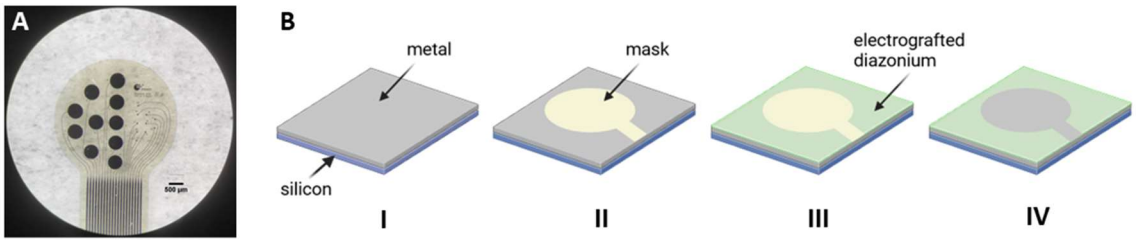

Figure 16. Image of a microelectrode array (the diameter of a single electrode d = 500 µm) (A). Scheme representing a micropatterning process using diazonium salts (B).

The concept of applying diazonium salts as biomedical coatings has been a subject of patent applications submitted into the Patent Office of the Republic of Poland under the titles *Bioactive biomedical coating and method of obtaining it*; registration no. **P.444428**, and *Method of obtaining a bioactive biomedical coating and bioactive biomedical coating*; registration no. **P.444429**.

4.3.3. Biofunctionalization

In the final attempt to utilize the diazonium salts, in **[A7]** we used them as anchoring points for bioactive molecules, namely poly-L-lysine (PLL), to enhance cell integration with the electrode (**Figure 17**). PLL is a polycationic molecule which can be used to promote cellular adhesion due to electrostatic interactions between the positively charged polymer chains and the negatively charged proteins and cell membrane components [102]. PLL is often used as a coating material for culture surfaces to enhance cell attachment and growth, particularly for adherent cell lines.

The methodology involved the electrografting of D-OCH_3, D-Cl_2, and D-NO_2. The latter was used to obtain nitrophenyl layer, followed by further electrochemical reduction to form a 4-aminophenyl (D-NH_2) layer on the electrode surface. PLL was then immobilized on the modified electrodes using two methods: drop casting and covalent coupling with a cross-linking agent – 1-ethyl-3-(3-dimethylaminopropyl)carbodiimide (EDC). The surface properties of the modified electrodes were characterized by Raman and FTIR spectroscopy, contact angle measurements, and electrochemical impedance spectroscopy to confirm the successful grafting of PLL and to assess the surface properties of the modified electrodes.

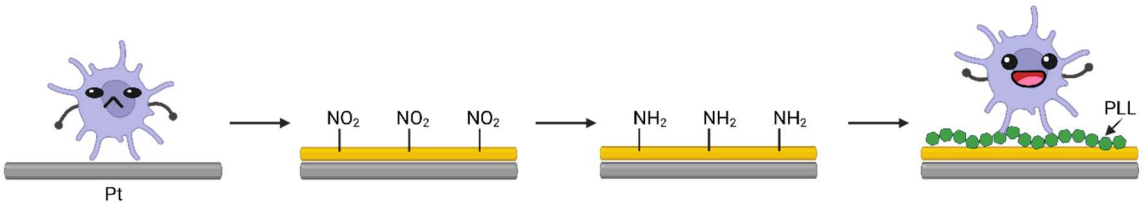

*Figure 17. Scheme representing the general concept of **[A7]**. By surface modification with diazonium salts and PLL the cell adhesion gets improved.*

SH-SY5Y neuroblastoma cell line was used to assess the influence of surface modifications on neural cell adhesion. In the protocol I developed, cells were cultured on PLL-modified electrodes for 1 hour, followed by washing to remove loosely attached cells. Images were taken to analyze cell attachment on diazonium-coated electrodes with and without PLL. Compared to fluorescent staining or dehydration of cells for SEM imaging, this method is much more straightforward and less time-consuming, while not requiring expensive reagents.

The diazonium electrografting process significantly increased cell attachment compared to a tissue culture plastic control, with the highest cell density observed on D-NH_2, showing a 3-fold increase (**Figure 18A**). PLL modification further enhanced cell attachment, with D-NH_2/PLL electrodes showing the most significant increase, indicating faster and more robust formation of adhesion complexes (**Figure 18B**). Cell attachment was notably lower on bare Pt/PLL electrodes compared to diazonium/PLL-modified surfaces, highlighting enhanced PLL immobilization on pre-functionalized electrodes. The simplified reaction scheme of covalent bonding of PLL to D-NH_2 is presented in **Figure 19**. Using EDC chemistry, the immobilization of PLL was improved and, therefore, D-NH_2/PLL exhibited the highest cell adhesion among all investigated samples. Notably, both diazonium and diazonium/PLL-modified electrodes supported the attachment of individual cells, whereas the unmodified Pt surface led to cell clustering. These results confirm that diazonium and diazonium/PLL-functionalized electrodes effectively promote SH-SY5Y cell adhesion on Pt-based electrodes.

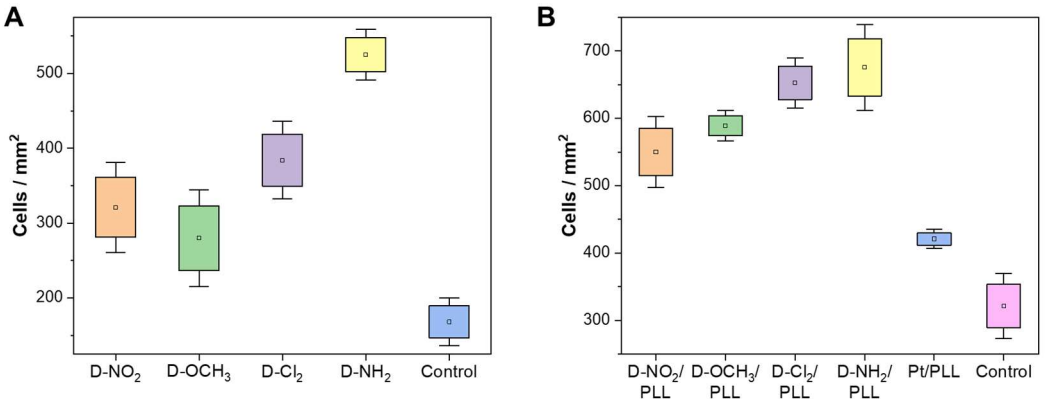

Figure 18. Cell adhesion studies on SH-SY5Y by Pt surface modification with electrografted diazonium salts (A) and by additional coating with PLL (B). The average number of cells per mm² is shown as a small square, the box represents the amplitude of the standard error, and the whiskers represent the 1.5 of the standard error.

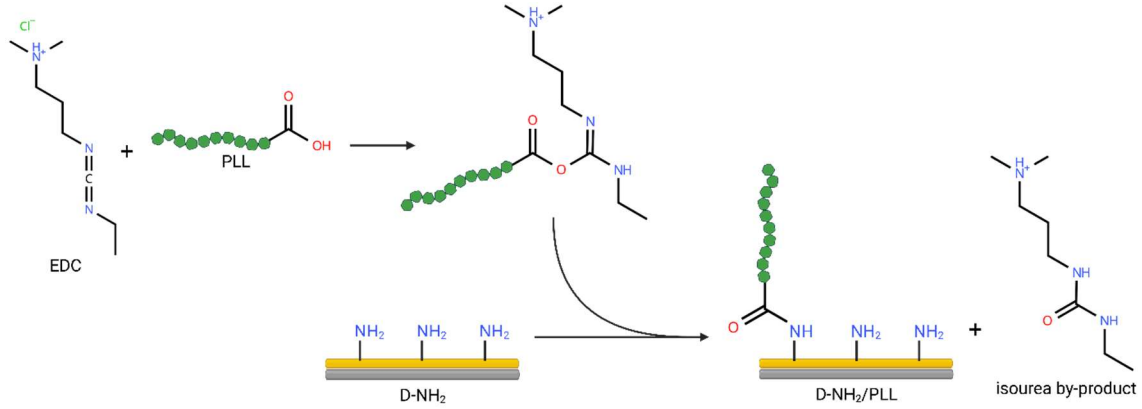

Figure 19. Simple scheme of amide coupling reaction between PLL and D-NH₂-functionalized Pt electrode using EDC.

The concept of applying diazonium salts coupled with bioactive molecules as biomedical coatings has been a subject of patent applications submitted into the Patent Office of the Republic of Poland under the titles *Polypeptide pro-adhesive coating and method of obtaining it*; registration no. **P.444427**, and *Biofunctionalized organic coating, method of its preparation and application*; registration no. **P.442508**.

In this chapter, I presented the versatility and effectiveness of surface functionalization approaches with the use of diazonium salts. Through electrochemical grafting of various diazonium salts onto platinum surfaces, significant improvements were achieved in adhesion, charge transfer, and mechanical stability of PEDOT:PSS coatings, as well as in the modulation of surface properties such as roughness, wettability, and conductivity. Moreover, mixed diazonium layers exhibited the ability to reduce bacterial adhesion without compromising mammalian cell compatibility. Further enhancement was achieved by coupling these modified

surfaces with PLL, resulting in a substantial increase in neuronal cell adhesion. Collectively, these studies present an innovative and adaptable surface functionalization approach, extending the applicability of CPs and metal electrodes in creating multifunctional interfaces in bioelectronics and biomedical engineering.

5. Summary

The findings presented in this thesis support the hypothesis that the proposed surface functionalization methods, whether applied individually or synergistically, can offer a powerful strategy to improve the performance of implantable bioelectronic interfaces. By selectively leveraging the unique benefits of each method, surface properties can be precisely tailored to address the specific requirements of diverse bioelectronic applications. A summary of the key conclusions from each study is presented below. The most significant conclusions are synthesized and presented in the following summary.

- Despite sharing the same polymer backbone, PEDOT electropolymerized with different counterions displayed distinct capacitive, morphological, and biological properties, highlighting the significant influence of dopant choice. PEDOT/PF_6 showed the highest electrochemical capacitance, while PEDOT/ClO_4 exhibited superior biocompatibility compared to the widely used PEDOT/PSS and bare platinum. The findings emphasize that dopant selection is a powerful tool for tuning PEDOT's performance in bioelectronic applications.
- By sequentially depositing gold and silver particles onto the surface of PEDOT, the resulting PEDOT-Au/Ag coating exhibited both electrochemical activity and antibacterial properties. The presence of gold particles helped mitigate the toxicity of silver towards mammalian cells, while preserving its antimicrobial effects, offering a promising approach for developing multifunctional materials suited for electroceutical and biomedical applications.
- PEDOT:Nafion films were found to serve as promising materials for biocompatible supercapacitor applications by demonstrating high areal and volumetric capacitance, low charge transfer resistance, and excellent ion diffusion. Solvent treatment was shown to further enhance charge carrier density by reducing film volume without affecting the total number charge carriers. A symmetric PEDOT:Nafion-based supercapacitor showed efficient performance, including high Coulombic efficiency and long-term stability.
- A layer-by-layer electrochemical polymerization was shown as a suitable approach to fabricate conducting polymer-based 3D materials for high-performance supercapacitors in bioelectronic applications. Resulting PEDOT/PEDOP hybrid structures showed superior performance compared to the individual homopolymers, PEDOT and PEDOP. The composite achieved highest areal capacitance, demonstrated the lowest charge transfer resistance and highest energy density among tested samples. The improved performance is attributed to the 3D structure formed when PEDOP polymerized over the PEDOT layer, enhancing the electrochemical surface area and ion transport.

- Diazonium chemistry was shown to be an effective method for enhancing the performance and expanding the applicability of PEDOT:PSS in organic bioelectronics. Surface modification of Pt electrode with diazonium salts created an organic layer that improved PEDOT:PSS adhesion. This modification reduced charge transfer resistance, increased capacitance, and enhanced the mechanical stability of the conducting polymer coating.
- Diazonium salts and their mixtures can be effective to create functionalized bioactive surfaces. The chemical character of the functional groups had a decisive effect on the physiochemical properties of electrografted layers, i.e. physicochemical (roughness, wettability), electrochemical (conductivity, capacitance) and biological properties. Particularly, as-formed organic layers were able to largely reduce bacterial adhesion without affecting biocompatibility towards eukaryotic cells. The charge blocking nature of the coatings, especially on micro-scale surfaces, could be useful for minimizing electrochemical interference in biosensing. This approach can be applicable to biomedical metals and alloys, with potential in neural, bone, and cardiovascular engineering.
- Diazonium salts can also be effectively used for enhancing neuronal cell attachment on Pt electrodes, especially when combining them with adhesion-promoting biomolecules such as PLL. Furthermore, this effect was improved due to covalent PLL immobilization through chemical coupling strategy, which could prove effective in enhancing integration of bioelectronic interfaces with neural tissue.

In conclusion, the methods presented in this work – each targeting specific aspects, such as electrochemical performance, biocompatibility, stability, or antibacterial properties – contribute to the growing library of surface functionalization strategies for bioelectronic devices. By offering tailored solutions to meet diverse functional requirements, these approaches support the development of more efficient and adaptable material interfaces. This work not only demonstrates my comprehensive expertise in electrochemical and surface characterization techniques but also reflects my ability to independently design and analyze cell culture experiments. My interdisciplinary competence, extending beyond the chemical sciences into biological studies, has been critical in ensuring the functional and biological relevance of the developed materials. Given the rapid growth of the bioelectronics market and its increasing demand for high-performance, biocompatible, and multifunctional materials, such advancements are particularly valuable for accelerating innovation in next-generation implantable bioelectronic devices.

6. Literature

[1] M. Skorupa, D. Więcławska, D. Czerwińska-Główka, M. Skonieczna, K. Krukiewicz, Dopant-Dependent Electrical and Biological Functionality of PEDOT in Bioelectronics, Polymers (Basel). 13 (2021) 1948. https://doi.org/10.3390/polym13121948.

[2] S. Smołka, M. Skorupa, K. Fołta, A. Banaś, K. Balcerzak, D. Krok, D.Y. Shyntum, M. Skonieczna, R. Turczyn, K. Krukiewicz, Antibacterial coatings for electroceutical devices based on PEDOT decorated with gold and silver particles, Bioelectrochemistry. 153 (2023) 108484. https://doi.org/10.1016/j.bioelechem.2023.108484.

[3] M. Skorupa, K. Karoń, E. Marchini, S. Caramori, S. Pluczyk-Małek, K. Krukiewicz, S. Carli, PEDOT:Nafion for Highly Efficient Supercapacitors, ACS Appl. Mater. Interfaces. 16 (2024) 23253–23264. https://doi.org/10.1021/acsami.4c01085.

[4] M. Skorupa, E. Cao, A. Barylski, S. Shakibania, S. Pluczyk-Małek, Z. Siwy, K. Krukiewicz, Layer-By-Layer Approach to Improve the Capacitance of Conducting Polymer Films, Adv. Electron. Mater. 2400761 (2025) 1–11. https://doi.org/10.1002/aelm.202400761.

[5] S. Smołka, M. Skorupa, A. Barylski, M. Basiaga, K. Krukiewicz, Improved adhesion and charge transfer between PEDOT:PSS and the surface of a platinum electrode through a diazonium chemistry route, Electrochem. Commun. 153 (2023) 107528. https://doi.org/10.1016/j.elecom.2023.107528.

[6] M. Skorupa, M. Skonieczna, D.Y. Shyntum, Abdullah, R. Turczyn, M. Asplund, K. Krukiewicz, Electrografted mixed organic monolayers as antibacterial coatings for implantable biomedical devices, Electrochim. Acta. 492 (2024) 144354. https://doi.org/10.1016/j.electacta.2024.144354.

[7] T. Patel, M. Skorupa, M. Skonieczna, R. Turczyn, K. Krukiewicz, Surface grafting of poly-L-lysine via diazonium chemistry to enhance cell adhesion to biomedical electrodes, Bioelectrochemistry. 152 (2023) 108465. https://doi.org/10.1016/j.bioelechem.2023.108465.

[8] F. Pesantez Torres, N. Tokranova, E. Amodeo, T. Bertucci, T.R. Kiehl, Y. Xie, N.C. Cady, S.T. Sharfstein, Interfacing neural cells with typical microelectronics materials for future manufacturing, Biosens. Bioelectron. 242 (2023) 115749. https://doi.org/10.1016/j.bios.2023.115749.

[9] S.G. Higgins, A. Lo Fiego, I. Patrick, A. Creamer, M.M. Stevens, Organic Bioelectronics: Using Highly Conjugated Polymers to Interface with Biomolecules, Cells, and Tissues in the Human Body, Adv. Mater. Technol. 5 (2020) 1–35. https://doi.org/10.1002/admt.202000384.

[10] M. Zamani, C.M. Klapperich, A.L. Furst, Recent advances in gold electrode fabrication for low-resource setting biosensing, Lab Chip. 23 (2023) 1410–1419. https://doi.org/10.1039/D2LC00552B.

[11] S. Bredeson, A. Kanneganti, F. Deku, S. Cogan, M. Romero-Ortega, P. Troyk, Chronic in-vivo testing of a 16-channel implantable wireless neural stimulator, in: 2015 37th Annu. Int. Conf. IEEE Eng. Med. Biol. Soc., IEEE, 2015: pp. 1017–1020. https://doi.org/10.1109/EMBC.2015.7318537.

[12] E.M. Hudak, D.W. Kumsa, H.B. Martin, J.T. Mortimer, Electron transfer processes occurring on platinum neural stimulating electrodes: Calculated charge-storage capacities are inaccessible during applied stimulation, J. Neural Eng. 14 (2017) 046012. https://doi.org/10.1088/1741-2552/aa6945.

[13] W. Duan, U.A. Robles, L. Poole-Warren, D. Esrafilzadeh, Bioelectronic Neural Interfaces: Improving Neuromodulation Through Organic Conductive Coatings, Adv. Sci. 11 (2024). https://doi.org/10.1002/advs.202306275.

[14] C. Vallejo-Giraldo, A. Kelly, M.J.P. Biggs, Biofunctionalisation of electrically conducting polymers, Drug Discov. Today. 19 (2014) 88–94. https://doi.org/10.1016/j.drudis.2013.07.022.

[15] D. Czerwińska-Główka, W. Przystaś, E. Zabłocka-Godlewska, S. Student, B. Cwalina, M. Łapkowski, K. Krukiewicz, Bacterial Surface Colonization of Sputter-Coated Platinum

Films, Materials (Basel). 13 (2020) 2674. https://doi.org/10.3390/ma13122674.
[16] S. Cai, C. Wu, W. Yang, W. Liang, H. Yu, L. Liu, Recent advance in surface modification for regulating cell adhesion and behaviors, Nanotechnol. Rev. 9 (2020) 971–989. https://doi.org/10.1515/ntrev-2020-0076.
[17] J. Kappen, M. Skorupa, K. Krukiewicz, Conducting Polymers as Versatile Tools for the Electrochemical Detection of Cancer Biomarkers, Biosensors. 13 (2022) 31. https://doi.org/10.3390/bios13010031.
[18] K. Krukiewicz, M. Chudy, C. Vallejo-Giraldo, M. Skorupa, D. Więcławska, R. Turczyn, M. Biggs, Fractal form PEDOT/Au assemblies as thin-film neural interface materials, Biomed. Mater. 13 (2018). https://doi.org/10.1088/1748-605X/aabced.
[19] G. Oyman, C. Geyik, R. Ayranci, M. Ak, D. Odaci Demirkol, S. Timur, H. Coskunol, Peptide-modified conducting polymer as a biofunctional surface: monitoring of cell adhesion and proliferation, RSC Adv. 4 (2014) 53411–53418. https://doi.org/10.1039/C4RA08481K.
[20] D. Khatayevich, M. Gungormus, H. Yazici, C. So, S. Cetinel, H. Ma, A. Jen, C. Tamerler, M. Sarikaya, Biofunctionalization of materials for implants using engineered peptides, Acta Biomater. 6 (2010) 4634–4641. https://doi.org/10.1016/j.actbio.2010.06.004.
[21] X. Liu, Z. Yue, M.J. Higgins, G.G. Wallace, Conducting polymers with immobilised fibrillar collagen for enhanced neural interfacing, Biomaterials. 32 (2011) 7309–7317. https://doi.org/10.1016/j.biomaterials.2011.06.047.
[22] G.D. Sulka, Electrochemistry of Thin Films and Nanostructured Materials, Molecules. 28 (2023) 4040. https://doi.org/10.3390/molecules28104040.
[23] C. Boehler, Z. Aqrawe, M. Asplund, Applications of PEDOT in bioelectronic medicine, Bioelectron. Med. 2 (2019) 89–99. https://doi.org/10.2217/bem-2019-0014.
[24] C. Boehler, D.M. Vieira, U. Egert, M. Asplund, NanoPt—A Nanostructured Electrode Coating for Neural Recording and Microstimulation, ACS Appl. Mater. Interfaces. 12 (2020) 14855–14865. https://doi.org/10.1021/acsami.9b22798.
[25] A.S. Bondarenko, G.A. Ragoisha, EIS Spectrum Analyser, in: Prog. Chemom. Res., Nova Science Publishers, New York, 2005: pp. 88–102.
[26] A. Ahnood, A. Chambers, A. Gelmi, K.-T. Yong, O. Kavehei, Semiconducting electrodes for neural interfacing: a review, Chem. Soc. Rev. 52 (2023) 1491–1518. https://doi.org/10.1039/D2CS00830K.
[27] T. V. Vernitskaya, O.N. Efimov, Polypyrrole: A conducting polymer (synthesis, properties, and applications), Usp. Khim. 66 (1997) 502–505. https://doi.org/10.1070/rc1997v066n05abeh000261.
[28] E. Poverenov, M. Li, A. Bitler, M. Bendikov, Major effect of electropolymerization solvent on morphology and electrochromic properties of PEDOT films, Chem. Mater. 22 (2010) 4019–4025. https://doi.org/10.1021/cm100561d.
[29] C. Bodart, N. Rossetti, J. Hagler, P. Chevreau, D. Chhin, F. Soavi, S.B. Schougaard, F. Amzica, F. Cicoira, Electropolymerized Poly(3,4-ethylenedioxythiophene) (PEDOT) Coatings for Implantable Deep-Brain-Stimulating Microelectrodes, ACS Appl. Mater. Interfaces. 11 (2019) 17226–17233. https://doi.org/10.1021/acsami.9b03088.
[30] M. Culebras, C.M. Gómez, A. Cantarero, Enhanced thermoelectric performance of PEDOT with different counter-ions optimized by chemical reduction, J. Mater. Chem. A. 2 (2014) 10109–10115. https://doi.org/10.1039/C4TA01012D.
[31] Y. Seki, M. Takahashi, M. Takashiri, Effects of different electrolytes and film thicknesses on structural and thermoelectric properties of electropolymerized poly(3,4-ethylenedioxythiophene) films, RSC Adv. 9 (2019) 15957–15965. https://doi.org/10.1039/c9ra02310k.
[32] L.C. Hsu, J. Fang, D.A. Borca-Tasciuc, R.W. Worobo, C.I. Moraru, Effect of micro- and nanoscale topography on the adhesion of bacterial cells to solid surfaces, Appl. Environ. Microbiol. 79 (2013) 2703–2712. https://doi.org/10.1128/AEM.03436-12.
[33] M. Solazzo, K. Krukiewicz, A. Zhussupbekova, K. Fleischer, M.J. Biggs, M.G. Monaghan, PEDOT:PSS interfaces stabilised using a PEGylated crosslinker yield improved conductivity and biocompatibility, J. Mater. Chem. B. 7 (2019) 4811–4820.

https://doi.org/10.1039/C9TB01028A.
[34] S.F. Cogan, Neural Stimulation and Recording Electrodes, Annu. Rev. Biomed. Eng. 10 (2008) 275–309. https://doi.org/10.1146/annurev.bioeng.10.061807.160518.
[35] P. Danielsson, J. Bobacka, A. Ivaska, Electrochemical synthesis and characterization of poly(3,4- ethylenedioxythiophene) in ionic liquids with bulky organic anions, J. Solid State Electrochem. 8 (2004) 809–817. https://doi.org/10.1007/s10008-004-0549-2.
[36] R. Kim, Y. Nam, Polydopamine-doped conductive polymer microelectrodes for neural recording and stimulation, J. Neurosci. Methods. 326 (2019) 108369. https://doi.org/10.1016/j.jneumeth.2019.108369.
[37] W. Shi, Q. Yao, W. Donghui, S. Qu, Y. Chen, K.H. Lee, L. Chen, Vapor phase polymerization of Ag QD-embedded PEDOT film with enhanced thermoelectric and antibacterial properties, NPG Asia Mater. 2022 141. 14 (2022) 1–8. https://doi.org/10.1038/s41427-022-00391-7.
[38] Y. Xu, J. Ma, Y. Han, H. Xu, Y. Wang, D. Qi, W. Wang, A simple and universal strategy to deposit Ag/polypyrrole on various substrates for enhanced interfacial solar evaporation and antibacterial activity, Chem. Eng. J. 384 (2020) 123379. https://doi.org/10.1016/J.CEJ.2019.123379.
[39] H.J. Park, S. Park, J. Roh, S. Kim, K. Choi, J. Yi, Y. Kim, J. Yoon, Biofilm-inactivating activity of silver nanoparticles: A comparison with silver ions, J. Ind. Eng. Chem. 19 (2013) 614–619. https://doi.org/10.1016/j.jiec.2012.09.013.
[40] A. Domínguez-Bajo, J.M. Rosa, A. González-Mayorga, B.L. Rodilla, A. Arché-Núñez, E. Benayas, P. Ocón, L. Pérez, J. Camarero, R. Miranda, M.T. González, J. Aguilar, E. López-Dolado, M.C. Serrano, Nanostructured gold electrodes promote neural maturation and network connectivity, Biomaterials. 279 (2021) 121186. https://doi.org/10.1016/j.biomaterials.2021.121186.
[41] A.G. Gristina, Biomaterial-Centered Infection: Microbial Adhesion Versus Tissue Integration, Science (80-.). 237 (1987) 1588–1595. https://doi.org/10.1126/SCIENCE.3629258.
[42] S. Hackenberg, A. Scherzed, M. Kessler, S. Hummel, A. Technau, K. Froelich, C. Ginzkey, C. Koehler, R. Hagen, N. Kleinsasser, Silver nanoparticles: evaluation of DNA damage, toxicity and functional impairment in human mesenchymal stem cells, Toxicol. Lett. 201 (2011) 27–33. https://doi.org/10.1016/J.TOXLET.2010.12.001.
[43] C. Greulich, S. Kittler, M. Epple, G. Muhr, M. Köller, Studies on the biocompatibility and the interaction of silver nanoparticles with human mesenchymal stem cells (hMSCs), Langenbeck's Arch. Surg. 394 (2009) 495–502. https://doi.org/10.1007/S00423-009-0472-1.
[44] C.A.R. Chapman, L. Wang, H. Chen, J. Garrison, P.J. Lein, E. Seker, Nanoporous Gold Biointerfaces: Modifying Nanostructure to Control Neural Cell Coverage and Enhance Electrophysiological Recording Performance, Adv. Funct. Mater. 27 (2017) 1604631. https://doi.org/10.1002/adfm.201604631.
[45] R. Shukla, V. Bansal, M. Chaudhary, A. Basu, R.R. Bhonde, M. Sastry, Biocompatibility of gold nanoparticles and their endocytotic fate inside the cellular compartment: a microscopic overview, Langmuir. 21 (2005) 10644–10654. https://doi.org/10.1021/LA0513712.
[46] D. Di Bella, J.P.S. Ferreira, R. de N.O. Silva, C. Echem, A. Milan, E.H. Akamine, M.H. Carvalho, S.F. Rodrigues, Gold nanoparticles reduce inflammation in cerebral microvessels of mice with sepsis, J. Nanobiotechnology. 19 (2021) 52. https://doi.org/10.1186/S12951-021-00796-6.
[47] X. Guan, L. Pan, Z. Fan, Flexible, Transparent and Highly Conductive Polymer Film Electrodes for All-Solid-State Transparent Supercapacitor Applications, Membranes (Basel). 11 (2021) 788. https://doi.org/10.3390/membranes11100788.
[48] M. Rajesh, C.J. Raj, R. Manikandan, B.C. Kim, S.Y. Park, K.H. Yu, A high performance PEDOT/PEDOT symmetric supercapacitor by facile in-situ hydrothermal polymerization of PEDOT nanostructures on flexible carbon fibre cloth electrodes, Mater. Today Energy. 6 (2017) 96–104. https://doi.org/10.1016/j.mtener.2017.09.003.
[49] Z. Zhao, G.F. Richardson, Q. Meng, S. Zhu, H.-C. Kuan, J. Ma, PEDOT-based composites

as electrode materials for supercapacitors, Nanotechnology. 27 (2016) 042001. https://doi.org/10.1088/0957-4484/27/4/042001.
[50] X. Jia, Y. Ge, L. Shao, C. Wang, G.G. Wallace, Tunable Conducting Polymers: Toward Sustainable and Versatile Batteries, ACS Sustain. Chem. Eng. 7 (2019) 14321–14340. https://doi.org/10.1021/acssuschemeng.9b02315.
[51] N.R. Chodankar, S. V. Karekar, M. Safarkhani, A.M. Patil, P.A. Shinde, R.B. Ambade, J. Kim, Y. Han, Y. Huh, A. al Ghaferi, E. Alhajri, Revolutionizing Implantable Technology: Biocompatible Supercapacitors as the Future of Power Sources, Adv. Funct. Mater. 2406819 (2024). https://doi.org/10.1002/adfm.202406819.
[52] L. Zhai, J. Duan, T. Lin, H. Shao, Recent advances in implantable batteries: Development and challenge, J. Alloys Compd. 979 (2024) 173551. https://doi.org/10.1016/j.jallcom.2024.173551.
[53] S. Wang, L. Wei, F. Wang, L. Wang, J. Mao, Advanced implantable energy storage for powering medical devices, EScience. (2025) 100409. https://doi.org/10.1016/j.esci.2025.100409.
[54] S. Liu, L. Kang, S.C. Jun, Challenges and Strategies toward Cathode Materials for Rechargeable Potassium-Ion Batteries, Adv. Mater. 33 (2021). https://doi.org/10.1002/adma.202004689.
[55] W. Raza, F. Ali, N. Raza, Y. Luo, K.H. Kim, J. Yang, S. Kumar, A. Mehmood, E.E. Kwon, Recent advancements in supercapacitor technology, Nano Energy. 52 (2018) 441–473. https://doi.org/10.1016/j.nanoen.2018.08.013.
[56] Q. Meng, K. Cai, Y. Chen, L. Chen, Research progress on conducting polymer based supercapacitor electrode materials, Nano Energy. 36 (2017) 268–285. https://doi.org/10.1016/j.nanoen.2017.04.040.
[57] Z. Wu, L. Li, J.M. Yan, X.B. Zhang, Materials Design and System Construction for Conventional and New-Concept Supercapacitors, Adv. Sci. 4 (2017). https://doi.org/10.1002/advs.201600382.
[58] Y. Wu, S.S. Nagane, P. Sitarik, S. Chhatre, J. Lee, D.C. Martin, Capacitive studies of electrodeposited PEDOT-maleimide, J. Mater. Chem. A. 10 (2022) 8440–8458. https://doi.org/10.1039/D2TA00347C.
[59] Y. Wen, J. Xu, Scientific Importance of Water-Processable PEDOT–PSS and Preparation, Challenge and New Application in Sensors of Its Film Electrode: A Review, J. Polym. Sci. Part A Polym. Chem. 55 (2017) 1121–1150. https://doi.org/10.1002/pola.28482.
[60] H. Shi, C. Liu, Q. Jiang, J. Xu, Effective Approaches to Improve the Electrical Conductivity of PEDOT:PSS: A Review, Adv. Electron. Mater. 1 (2015) 1–16. https://doi.org/10.1002/aelm.201500017.
[61] S. Carli, M. Bianchi, M. Di Lauro, M. Prato, A. Toma, M. Leoncini, A. De Salvo, M. Murgia, L. Fadiga, F. Biscarini, Multifunctionally-doped PEDOT for organic electrochemical transistors, Front. Mater. 9 (2022) 1–15. https://doi.org/10.3389/fmats.2022.1063763.
[62] A.I. Hofmann, I. Östergren, Y. Kim, S. Fauth, M. Craighero, M.-H. Yoon, A. Lund, C. Müller, All-Polymer Conducting Fibers and 3D Prints via Melt Processing and Templated Polymerization, ACS Appl. Mater. Interfaces. 12 (2020) 8713–8721. https://doi.org/10.1021/acsami.9b20615.
[63] S. Carli, M. Di Lauro, M. Bianchi, M. Murgia, A. De Salvo, M. Prato, L. Fadiga, F. Biscarini, Water-Based PEDOT:Nafion Dispersion for Organic Bioelectronics, ACS Appl. Mater. Interfaces. 12 (2020) acsami.0c06538. https://doi.org/10.1021/acsami.0c06538.
[64] E. Marchini, M. Orlandi, N. Bazzanella, R. Boaretto, V. Cristino, A. Miotello, S. Caramori, S. Carli, Electrodeposited PEDOT/Nafion as Catalytic Counter Electrodes for Cobalt and Copper Bipyridyl Redox Mediators in Dye-Sensitized Solar Cells, ACS Omega. 7 (2022) 29181–29194. https://doi.org/10.1021/acsomega.2c03229.
[65] S. Guzzo, S. Carli, B. Pavan, A. Lunghi, M. Murgia, M. Bianchi, Evaluation of the In Vitro Biocompatibility of PEDOT:Nafion Coatings, Nanomaterials. 11 (2021) 2022. https://doi.org/10.3390/nano11082022.
[66] S. Sharma, R. Adalati, M. Sharma, S. Jindal, A. Kumar, G. Malik, R. Chandra, Single-step

fabrication of di-titanium nitride thin-film flexible and biocompatible supercapacitor, Ceram. Int. 48 (2022) 34678–34687. https://doi.org/10.1016/j.ceramint.2022.08.055.
[67] K. Krukiewicz, T. Jarosz, A.P. Herman, R. Turczyn, S. Boncel, J.K. Zak, The effect of solvent on the synthesis and physicochemical properties of poly(3,4-ethylenedioxypyrrole), Synth. Met. 217 (2016) 231–236. https://doi.org/10.1016/j.synthmet.2016.04.005.
[68] K. Krukiewicz, D. Kobus, R. Turczyn, K. Erfurt, A. Chrobok, M.J.P. Biggs, Low resistance, highly corrugated structures based on poly(3,4-ethylenedioxythiophene) doped with a d-glucopyranoside-derived ionic liquid, Electrochem. Commun. 110 (2020) 106616. https://doi.org/10.1016/j.elecom.2019.106616.
[69] K. Krukiewicz, A. Kowalik, D. Czerwinska-Glowka, M.J.P. Biggs, Electrodeposited poly(3,4-ethylenedioxypyrrole) films as neural interfaces: Cytocompatibility and electrochemical studies, Electrochim. Acta. 302 (2019) 21–30. https://doi.org/10.1016/j.electacta.2019.02.023.
[70] K. Krukiewicz, B. Gniazdowska, T. Jarosz, A.P. Herman, S. Boncel, R. Turczyn, Effect of immobilization and release of ciprofloxacin and quercetin on electrochemical properties of poly(3,4-ethylenedioxypyrrole) matrix, Synth. Met. 249 (2019) 52–62. https://doi.org/10.1016/j.synthmet.2019.02.001.
[71] D. Czerwińska-Główka, M. Skonieczna, A. Barylski, S. Golba, W. Przystaś, E. Zabłocka-Godlewska, S. Student, B. Cwalina, K. Krukiewicz, Bifunctional conducting polymer matrices with antibacterial and neuroprotective effects, Bioelectrochemistry. 144 (2022) 108030. https://doi.org/10.1016/j.bioelechem.2021.108030.
[72] A. Kumar, R.K. Singh, H.K. Singh, P. Srivastava, R. Singh, Enhanced capacitance and stability of p-toluenesulfonate doped polypyrrole/carbon composite for electrode application in electrochemical capacitors, J. Power Sources. 246 (2014) 800–807. https://doi.org/10.1016/j.jpowsour.2013.07.121.
[73] I. Beyers, A. Bensmann, R. Hanke-Rauschenbach, Ragone plots revisited: A review of methodology and application across energy storage technologies, J. Energy Storage. 73 (2023) 109097. https://doi.org/10.1016/j.est.2023.109097.
[74] M. Bianchi, S. Carli, M. Di Lauro, M. Prato, M. Murgia, L. Fadiga, F. Biscarini, Scaling of capacitance of PEDOT:PSS: volume vs. area, J. Mater. Chem. C. 8 (2020) 11252–11262.
[75] H. Mousavi, L.M. Ferrari, A. Whiteley, E. Ismailova, Kinetics and Physicochemical Characteristics of Electrodeposited PEDOT:PSS Thin Film Growth, Adv. Electron. Mater. 9 (2023). https://doi.org/10.1002/aelm.202201282.
[76] R.A. Green, R.T. Hassarati, L. Bouchinet, C.S. Lee, G.L.M. Cheong, J.F. Yu, C.W. Dodds, G.J. Suaning, L.A. Poole-Warren, N.H. Lovell, Substrate dependent stability of conducting polymer coatings on medical electrodes, Biomaterials. 33 (2012) 5875–5886. https://doi.org/10.1016/j.biomaterials.2012.05.017.
[77] L. Ouyang, B. Wei, C. Kuo, S. Pathak, B. Farrell, D.C. Martin, Enhanced PEDOT adhesion on solid substrates with electrografted P(EDOT-NH 2), Sci. Adv. 3 (2017) e1600448. https://doi.org/10.1126/sciadv.1600448.
[78] C. Boehler, F. Oberueber, S. Schlabach, T. Stieglitz, M. Asplund, Long-Term Stable Adhesion for Conducting Polymers in Biomedical Applications: IrOx and Nanostructured Platinum Solve the Chronic Challenge, ACS Appl. Mater. Interfaces. 9 (2017) 189–197. https://doi.org/10.1021/acsami.6b13468.
[79] Z. Huang, P.-C. Wang, A.G. MacDiarmid, Y. Xia, G. Whitesides, Selective Deposition of Conducting Polymers on Hydroxyl-Terminated Surfaces with Printed Monolayers of Alkylsiloxanes as Templates, Langmuir. 13 (1997) 6480–6484. https://doi.org/10.1021/la970537z.
[80] S. Samanta, I. Bakas, A. Singh, D.K. Aswal, M.M. Chehimi, In Situ Diazonium-Modified Flexible ITO-Coated PEN Substrates for the Deposition of Adherent Silver–Polypyrrole Nanocomposite Films, Langmuir. 30 (2014) 9397–9406. https://doi.org/10.1021/la501909r.
[81] M. Lo, R. Pires, K. Diaw, D. Gningue-Sall, M.A. Oturan, J.-J. Aaron, M.M. Chehimi, Diazonium Salts: Versatile Molecular Glues for Sticking Conductive Polymers to Flexible Electrodes, Surfaces. 1 (2018) 43–58. https://doi.org/10.3390/surfaces1010005.
[82] E. Villemin, B. Lemarque, T.T. Vũ, V.Q. Nguyen, G. Trippé-Allard, P. Martin, P.C. Lacaze,

J.C. Lacroix, Improved adhesion of poly(3,4-ethylenedioxythiophene) (PEDOT) thin film to solid substrates using electrografted promoters and application to efficient nanoplasmonic devices, Synth. Met. 248 (2019) 45–52. https://doi.org/10.1016/j.synthmet.2018.12.010.
[83] D. Chhin, D. Polcari, C.B.-L. Guen, G. Tomasello, F. Cicoira, S.B. Schougaard, Diazonium-Based Anchoring of PEDOT on Pt/Ir Electrodes via Diazonium Chemistry, J. Electrochem. Soc. 165 (2018) G3066–G3070. https://doi.org/10.1149/2.0061812jes.
[84] X. Zhang, W. Yang, H. Zhang, M. Xie, X. Duan, PEDOT:PSS: From conductive polymers to sensors, Nanotechnol. Precis. Eng. 4 (2021) 045004. https://doi.org/10.1063/10.0006866.
[85] J. Lipus, K. Krukiewicz, Challenges and limitations of using charge storage capacity to assess capacitance of biomedical electrodes, Measurement. 191 (2022) 110822. https://doi.org/10.1016/J.MEASUREMENT.2022.110822.
[86] S. Pandit, S. Kundu, Optical activity of polyelectrolyte (PSS) - Protein (lysozyme) complexes, AIP Conf. Proc. 2115 (2019) 030037.
[87] R.R. Smith, A.P. Smith, J.T. Stricker, B.E. Taylor, M.F. Durstock, Layer-by-Layer Assembly of Poly(3,4-ethylenedioxythiophene):Poly(styrenesulfonate), Macromolecules. 39 (2006) 6071–6074.
[88] S. Bouden, J. Pinson, C. Vautrin-Ul, Electrografting of diazonium salts: A kinetics study, Electrochem. Commun. 81 (2017) 120–123. https://doi.org/10.1016/j.elecom.2017.06.007.
[89] J.K. Kariuki, M.T. McDermott, Formation of multilayers on glassy carbon electrodes via the reduction of diazonium salts, Langmuir. 17 (2001) 5947–5951. https://doi.org/10.1021/la010415d.
[90] M. Fau, A. Kowalczyk, P. Olejnik, A.M. Nowicka, Tight and Uniform Layer of Covalently Bound Aminoethylophenyl Groups Perpendicular to Gold Surface for Attachment of Biomolecules, Anal. Chem. 83 (2011) 9281–9288. https://doi.org/10.1021/ac201794m.
[91] J. CarvalhoPadilha, J.M. Noël, J.F. Bergamini, J. Rault-Berthelot, C. Lagrost, Functionalization of Carbon Materials by Reduction of Diazonium Cations Produced in Situ in a Brønstedt Acidic Ionic Liquid, ChemElectroChem. 3 (2016) 572–580. https://doi.org/10.1002/CELC.201500434.
[92] X. Zhao, L. Jin, H. Shi, W. Tong, D. Gorin, Y. Kotelevtsev, Z. Mao, Recent advances of designing dynamic surfaces to regulate cell adhesion, Colloid Interface Sci. Commun. 35 (2020) 100249. https://doi.org/10.1016/j.colcom.2020.100249.
[93] K. Yang, J. Shi, L. Wang, Y. Chen, C. Liang, L. Yang, L. Wang, Bacterial anti-adhesion surface design: Surface patterning, roughness and wettability: A review, J. Mater. Sci. Technol. 99 (2022) 82–100. https://doi.org/10.1016/j.jmst.2021.05.028.
[94] International Organization for Standardization. (2009), Biological evaluation of medical devices — Part 5: Tests for in vitro cytotoxicity, (n.d.).
[95] J. Kim, R. Ghaffari, D.-H. Kim, The quest for miniaturized soft bioelectronic devices, Nat. Biomed. Eng. 1 (2017) 0049. https://doi.org/10.1038/s41551-017-0049.
[96] H.J. Lee, Y. Son, J. Kim, C.J. Lee, E.-S. Yoon, I.-J. Cho, A multichannel neural probe with embedded microfluidic channels for simultaneous in vivo neural recording and drug delivery, Lab Chip. 15 (2015) 1590–1597. https://doi.org/10.1039/C4LC01321B.
[97] T. Stieglitz, T. Boretius, J. Ordonez, C. Hassler, C. Henle, W. Meier, D.T.T. Plachta, M. Schuettler, Miniaturized neural interfaces and implants, in: H. Becker, B.L. Gray (Eds.), Microfluid. BioMEMS, Med. Microsystems X, 2012: p. 82510A. https://doi.org/10.1117/12.912526.
[98] M.D. Raicopol, C. Andronescu, R. Atasiei, A. Hanganu, E. Vasile, A.M. Brezoiu, L. Pilan, Organic layers via aryl diazonium electrochemistry: Towards modifying platinum electrodes for interference free glucose biosensors, Electrochim. Acta. 206 (2016). https://doi.org/10.1016/j.electacta.2016.04.145.
[99] M. Skorupa, T. Patel, K. Krukiewicz, Diazonium chemistry as a robust approach for the biofunctionalization of titanium surface, in: Recent Adv. Comput. Oncol. Pers. Med., 2022: p. 265. https://doi.org/10.34918/85101.
[100] M.A. Mezour, Y. Oweis, A.A. El-Hadad, S. Algizani, F. Tamimi, M. Cerruti, Surface modification of CoCr alloys by electrochemical reduction of diazonium salts, RSC Adv. 8 (2018) 23191–23198. https://doi.org/10.1039/C8RA02634C.

[101] X.T. Le, G. Zeb, P. Jégou, T. Berthelot, Electrografting of stainless steel by the diazonium salt of 4-aminobenzylphosphonic acid, Electrochim. Acta. 71 (2012) 66–72. https://doi.org/10.1016/j.electacta.2012.03.076.
[102] J.S. Heo, H.O. Kim, S.Y. Song, D.H. Lew, Y. Choi, S. Kim, Poly-L-lysine Prevents Senescence and Augments Growth in Culturing Mesenchymal Stem Cells Ex Vivo, Biomed Res. Int. 2016 (2016) 1–13. https://doi.org/10.1155/2016/8196078.

Summary of personal contribution

[A1] Contribution: optimization of electrochemical polymerization; investigation of electrochemical properties; EIS equivalent circuit fitting, description and visualization of results; surface characterization with SEM, description and analysis of results; analysis, description and visualization of in vitro experiments; writing and editing of the original draft.
My overall contribution to this research was equal to 40%.

[A2] Contribution: contact angle investigation, cell cytotoxicity investigation, methodology and formal analysis, writing – original draft.
My overall contribution to this research was equal to 20%.

[A3] Contribution: electrochemical properties investigation and analysis of results, visualization, writing of the original draft.
My overall contribution to this research was equal to 40%.

[A4] Contribution: conceptualization, optimization of electrochemical polymerization, electrochemical characterization, calculations and analysis of results, description of FIB-SEM, EDS and AFM results, investigation and analysis of FTIR results, description of scratch test results, preparation of all graphs and tables, writing of the original draft, funding acquisition.
My overall contribution to this research was equal to 65%.

[A5] Contribution: investigation and optimization of electrografting of diazonium salts, methodology of electrochemical experiments, validation, writing – original draft, supervision.
My overall contribution to this research was equal to 30%.

[A6] Contribution: optimization of electrografting, electrochemical characterization and analysis of results, description of XPS results, contact angle investigation and results analysis, profilometer measurements and results analysis, cell cytotoxicity investigation and results analysis, description of bacterial studies results, functionalization of microelectrodes and analysis of electrochemical results, preparation of all graphs and tables, writing of the original draft, funding acquisition.
My overall contribution to this research was equal to 65%.

[A7] Contribution: methodology and investigation of cell adhesion studies, editing of the manuscript.
My overall contribution to this research was equal to 20%.

List of scientific accomplishments

I. Publications and chapters other than those included in the thesis

1. K. Krukiewicz, J. Britton, D. Więcławska, **M. Skorupa**, J. Fernandez, J.R. Sarasua, M.J.P. Biggs, Electrical percolation in extrinsically conducting, poly(ε-decalactone) composite neural interface materials, Sci. Rep. 11 (2021) 1–10. https://doi.org/10.1038/s41598-020-80361-7.
2. J. Kappen, **M. Skorupa**, K. Krukiewicz, Conducting Polymers as Versatile Tools for the Electrochemical Detection of Cancer Biomarkers, Biosensors. 13 (2022) 31. https://doi.org/10.3390/bios13010031.
3. M. Śmiga-Matuszowicz, J. Włodarczyk, **M. Skorupa**, D. Czerwińska-Główka, K. Fołta, M. Pastusiak, M. Adamiec-Organiściok, M. Skonieczna, R. Turczyn, M. Sobota, K. Krukiewicz, Biodegradable Scaffolds for Vascular Regeneration Based on Electrospun Poly(L-Lactide-co-Glycolide)/Poly(Isosorbide Sebacate) Fibers, Int. J. Mol. Sci. 24 (2023) 1190. https://doi.org/10.3390/ijms24021190.
4. **M. Skorupa**, T. Patel, K. Krukiewicz, Diazonium chemistry as a robust approach for the biofunctionalization of titanium surface, in: Recent Adv. Comput. Oncol. Pers. Med., 2022: p. 265. https://doi.org/10.34918/85101.
5. K. Krukiewicz, M. Chudy, C. Vallejo-Giraldo, **M. Skorupa**, D. Więcławska, R. Turczyn, M. Biggs, Fractal form PEDOT/Au assemblies as thin-film neural interface materials, Biomed. Mater. 13 (2018). https://doi.org/10.1088/1748-605X/aabced.*
6. K. Krukiewicz, J. Fernandez, **M. Skorupa**, D. Więcławska, A. Poudel, J.-R. Sarasua, L.R. Quinlan, M.J.P. Biggs, Analysis of a poly(ε-decalactone)/silver nanowire composite as an electrically conducting neural interface biomaterial, BMC Biomed. Eng. 1 (2019). https://doi.org/10.1186/s42490-019-0010-3.*

* These publications were published before the start of my PhD.

II. Conferences

1. UK-Poland Bioinspired Materials Conference, 23-24.11.2020, MS Teams; poster presentation: *Influence of doping ions on the properties of PEDOT and its potential biomedical applications*.
2. 72nd Annual Meeting of the International Society of Electrochemistry (ISE), 29.08-03.09.2021, Jeju, South Korea; oral presentation: *Biofunctionalization of Electrodes for Bioelectronic Applications.*

3. Silesian Meetings on Polymer Materials POLYMAT2022, 17.03.2022, Zabrze, Poland; poster presentation: *Characterization of PEDOT properties relevant in bioelectronic applications.*
4. Computational Oncology and Personalized Medicine: The Challenges of the Future (COPM'2022), 27.04.2022, online; poster presentation: *Copolymerization of biocompatible conducting polymers: PEDOT/PEDOP.*
5. XXVII International Symposium on Bioelectrochemistry and Bioenergetics (BES2022), 03-07.04.2022, Antwerp, Belgium; poster presentation: *Biofunctionalization of neural electrodes with electroactive organic monolayers.*
6. 32nd Annual Conference of the European Society for Biomaterials (ESB2022), 04-08.09.2022, Bordeaux, France; poster presentation: *Homogeneous and Mixed Organic Monolayers as Coatings for Neural Interfaces*.
7. Computational Oncology and Personalized Medicine - Crossing Borders, Connecting Science (COPM2023), 26.04.2023, online; oral presentation: *Homogeneous and mixed organic monolayers as antibacterial biomedical coatings*.
8. 33rd Annual Conference of the European Society for Biomaterials (ESB2023), 4.09-8.09.2023, Davos, Switzerland; poster presentation: *Poly(L-lactide-co-glycolide)/poly(isosorbide sebacate) electrospun fibers as a biodegradable platform for vascular regeneration*.
9. 75th Annual Meeting of the International Society of Electrochemistry (ISE), 18-23.08.2024, Montréal, Canada; oral presentation: *Bilayer conducting polymer structures for supercapacitive applications*; poster presentation: *PEDOT:Nafion as a highly efficient alternative to PEDOT:PSS for energy storage applications*.

III. Research projects

1. 11.2020-07.2023: scholarship holder in a project *Biofunctionalized organic coatings as neuroelectronic interfaces* at the Silesian University of Technology (SUT), 2019/35/B/ST5/00995, National Science Centre Poland (NCN), within the OPUS framework.
2. 05.2021-12.2021: project manager in a project *Research on the possibility of copolymerization of conductive polymers: PEDOT/PEDOP*, 04/040/BKM21/0162, SUT internal research grant.
3. 04.2023-07.2023: participant in a project *Organic Charge Transfer Applications* (OCTA), SUT, under the European Union's Horizon 2020 (778158).
4. 10.2023-06.2024: participant in a project *PartNETships: a network of key collaborations to bring research excellence to the Silesian University of Technology*,

BPI/PST/2021/1/00039, Polish National Agency for Academic Exchange within the Strategic Partnerships program.

5. 08.2024-12.2024: scholarship holder in a project *Multilayer electroactive coatings with hierarchical structure for controlled delivery of neurotransmitters*, SUT, 2021/42/E/ST5/00165, NCN, within the SONATA-BIS framework.

IV. Internships

1. Germany, University of Freiburg, BrainLinks-BrainTools Centre, 14.09-13.12.2022, under the supervision of Prof. Maria Asplund.
2. New Zealand, University of Auckland, Advanced Polymer Research group, 17.04-16.07.2023, under the supervision of Prof. Jadranka Travaš-Sejdić.
3. USA, University of California Irvine, Siwy Research Lab, 15-31.10.2023, under the supervision of Prof. Zuzanna Siwy.
4. USA, University of California Irvine, Siwy Research Lab, 17.04-01.05.2024, under the supervision of Prof. Zuzanna Siwy.

V. Other

1. Rector's scholarship for the best doctoral students of SUT under the Excellence Initiative – Research University program, awarded for the academic years 2021/2022 and 2023/2024.
2. Co-supervision of 3 Project Based Learning (PBL) student projects at SUT (2021/2022, 2022/2023 and 2023/2024).
3. Pro-quality grant for at least 3-month internship in leading foreign research centers under the Excellence Initiative – Research University program, 32/014/SDU/10-27-04.
4. Master thesis co-supervision: *Biofunctionalization of neuroelectronic electrode surfaces*, Anna Krzak, 2021.

Appendix